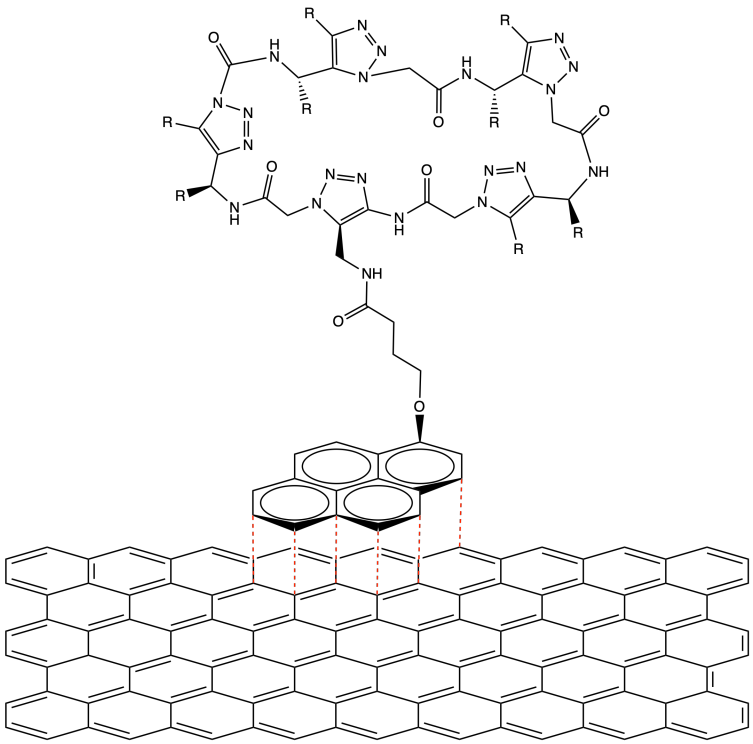

Non-covalent linking of synthetic receptors to graphene for biosensor applications

Master's thesis in Materials Chemistry

MARILOU BAGGE

DEPARTMENT OF CHEMISTRY AND CHEMICAL ENGINEERING

CHALMERS UNIVERSITY OF TECHNOLOGY
Gothenburg, Sweden 2022
www.chalmers.se

Master's thesis 2022

Non-covalent linking of synthetic receptors to graphene for biosensor applications

MARILOU BAGGE

CHALMERS
UNIVERSITY OF TECHNOLOGY

Department of Chemistry and Chemical Engineering
Division of Chemistry and Biochemistry
Chalmers University of Technology
Gothenburg, Sweden 2022

Non-covalent linking of synthetic receptors to graphene for biosensor applications
MARILOU BAGGE

Supervisor: Nina Kann, Department of Chemistry and Chemical Engineering
Supervisor: Flavia Ferrara, Department of Chemistry and Chemical Engineering
Examiner: Xiaoyan Zhang, Department of Chemistry and Chemical Engineering

Master's Thesis 2022
Department of Chemistry and Chemical Engineering
Division of Chemistry and Biochemistry
Chalmers University of Technology
SE-412 96 Gothenburg
Telephone +46 31 772 1000

Cover: A general synthetic receptor of cyclized triazole units linked to a graphene surface via non-covalent interactions.

Typeset in LaTeX
Printed by Chalmers Reproservice
Gothenburg, Sweden 2022

Non-covalent linking of synthetic receptors to graphene for biosensor applications
MARILOU BAGGE
Department of Chemistry and Chemical Engineering
Chalmers University of Technology

Abstract

Pathogenic infections pose a major risk for human health and a large part of the world's population do not receive the medical attention that they need due to unavailable diagnostic equipment. It is of interest to develop new rapid, inexpensive and highly sensitive analytical devices to detect and treat bacterial infections in time. Development of synthetic biosensors, specifically graphene-based biosensors to recognize biomarkers of the bacterial infections has progressed significantly the past years. The scope of the extensive EU-project PEST BIN is to develop a biosensor consisting of a synthetic receptor, an aromatic linker chain and a graphene-coated chip. This Master's thesis specifically investigated the aromatic linker chain between the synthetic receptor and the graphene surface. Also, a few synthetic routes utilizing click-chemistry to produce triazoles were evaluated.

Aromatic units of different size connected to a short linker chain were prepared by *O*-alkylation. The obtained aromatic compounds were analyzed and functionalized on a graphene-coated EVA/PET chip. It was desired to attach the aromatic linker to the graphene via non-covalent interactions and then examine the binding efficiency by Hall-effect measurements and Raman spectroscopy. Additionally, several triazole units were prepared by ruthenium- or copper-catalyzed azide alkyne cycloaddition (RuAAC and CuAAC) reactions. The triazole units were synthesized to ultimately link them to the aromatic units to obtain a simplified receptor model by attaching it to the graphene surface.

Phenols and naphthols - the simplest polycyclic aromatic hydrocarbon (PAH) - were alkylated with a propyl group, as a short model for the polyethylene glycol chain (PEG). Several alkylated naphthols were obtained successfully by the selected synthesis method, while no alkylated phenols were obtained. Further, the derivatized aromatic linkers were functionalized on the graphene surface. It was not possible to confirm if the compounds had interacted with the graphene by non-covalent interactions when analyzing the obtained results. Furthermore, some triazole units were obtained successfully from the performed click-reactions. However, a simple receptor model consisting of the aromatic unit and a single triazole was not obtained in this project, thus how the triazole functionality affects the graphene could not be determined, but requires further studies.

Keywords: Biosensor, synthetic receptor, graphene, alkylated aromatic compound, linker chain, functionalization

Acknowledgements

I would like to extend my gratitude to my supervisor Nina Kann who has been a great support and provided valuable and interesting ideas about the project in our daily meetings. Professor Kann has been available for discussion and helped with all challenges I have faced throughout my thesis, regardless if it's been about the laboratory, or the report. Additionally, I am grateful for have been given the opportunity to participate in the extensive EU-funded project PEST BIN.

I would like to thank my co-supervisor Flavia Ferrara who has always been available for discussion and guidance in my daily laboratory work. I would also like to thank our collaborator and PhD student Munis Khan at the department of Microtechnology and Nanoscience (MC2) who gave me a guided tour of the MC2 department. I want to thank our collaborator August Yurgens who provided valuable knowledge about quantum device physics which helped the project go forward. Additionally, I would like to thank Master's student Abdinasir Fahran Ahmed and Bachelor's student Kevin van Zitteren for daily collaboration and discussion in the laboratory.

Lastly, I would like to thank my examiner Xiaoyan Zhang for sharing interesting thoughts on the topic and provided me with great feedback and discussion which allowed me to improve my thesis further.

Marilou Bagge, Gothenburg, June 2022

Abbreviations

CuAAC	Copper-catalyzed azide alkyne cycloaddition
CVD	Chemical vapor deposition
EVA	Ethylene vinyl acetate
NMR	Nuclear magnetic resonance
NOESY	Nuclear Overhauser effect spectroscopy
S_N2	Nucleofilic substitution
PEG	Polyethylene glycol-based linker chain
PET	Polyethylene terephthalate
TLC	Thin layer chromatography
RuAAC	Ruthenium-catalyzed azide alkyne cycloaddition

Nomenclature

Boc	*tert*-Butyloxycarbonyl protecting group
DCM	Dichloromethane
DIPEA	*N,N*-Diisopropylethylamine
DMF	Dimethylformamide
EtOAc	Ethyl acetate
HATU	Hexafluorophosphate azabenzotriazole tetramethyl uronium
Me-THF	Methyltetrahydrofuran
Na_2SO_4	Sodium sulfate
OH	Hydroxy group
PAH	Poly aromatic hydrocarbon
PBASE	1-Pyrenebutyric acid *N*-hydroxysuccinimide ester
THF	Tetrahydrofuran

Contents

1
Introduction

Infections caused by pathogens are a major problem and poses a high risk for human health. A large part of the world's population is affected by bacterial diseases and do not receive the medical attention that they need [1]. As a result, millions of people die worldwide every year because of the pathogens, a group of microorganisms including bacteria and viruses, which can cause harmful infections. Hence, it is of importance to have a primary health care, providing the right medical techniques to detect the pathogenic diseases and receive proper treatment. Today's most common analytical techniques are the polymerase chain reaction (PCR) and enzyme-linked immunosorbent assay (ELISA) which have the advantages of high sensitivity. On the contrary, these detection techniques require expensive and professional equipment and the processes are very time-consuming [2]. Also, hospitals in many countries and cities do not have access to highly technological and expensive instruments, especially in developing countries [3][4]. Therefore, it is of interest to develop new rapid, highly sensitive and inexpensive analytical devices to recognize the bacterial infections as a complementary detection technique.

Within the scope of medical diagnostics, nano-technological biosensors are being developed for detecting biomarkers to indicate bacterial infections. In recent years, the ability to design small synthetic receptors with the capability to bind to specific biomarkers such as amino acids and peptides has progressed significantly [5]. Specifically, graphene-based biosensors have been developed extensively during the past years [2]. The end goal is to create inexpensive biosensors which are portable and easy to use. Thus, by implementing these devices and distributing them to hospitals all over the world, it would enable accurate diagnosis and rapid treatment of diseases. As a result, human health would improve which is of great benefit in societal aspects.

This Master's thesis is part of an extensive EU-funded project, PEST BIN, that focuses on further developments of biosensor applications. The project is in collaboration with researchers at B, K, MC2 at Chalmers University of Technology and Sahlgrenska. The large scope of this project is to develop a complete biosensor which will consist of a synthetic receptor attached to an aromatic linker chain which in turn is bound to a graphene-coated chip as shown in Figure 1.1. The function of the device is to produce a signal when a certain bacterial infection is encountered.

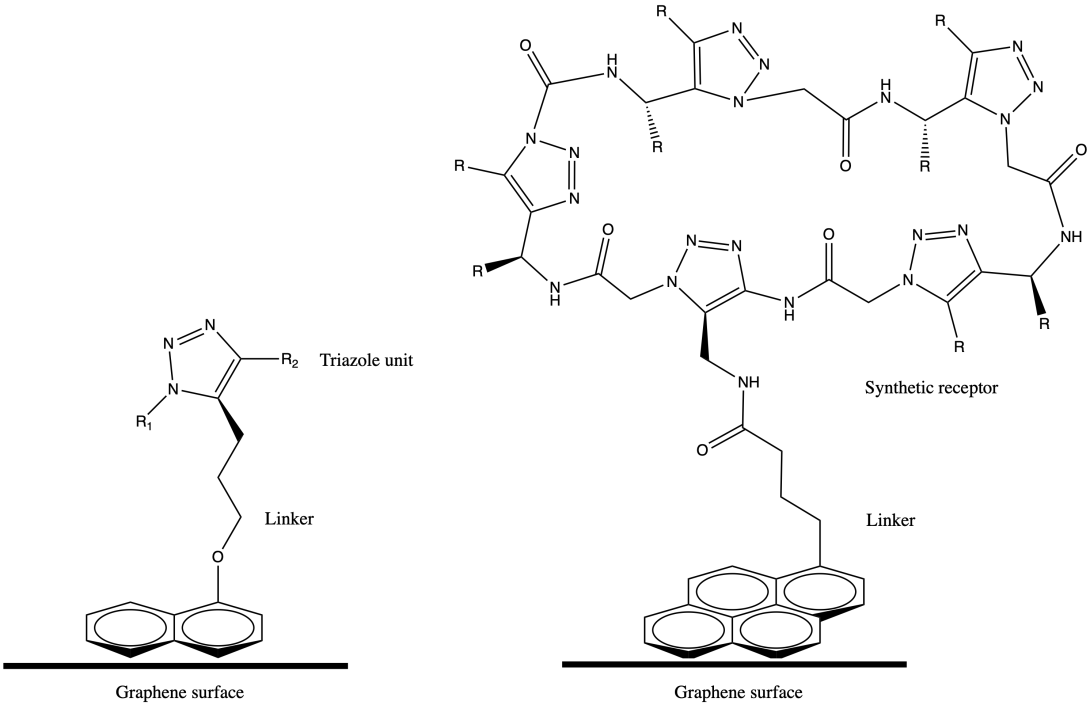

Figure 1.1: The first illustration represents a proposed single triazole unit attached to a simple aromatic linker chain bound to the graphene surface. The second illustration represents a general synthetic receptor attached to a pyrene aromatic linker chain bound to the graphene surface.

1.1 Aim and scope

The aim of this Master's thesis is to develop an aromatic linker chain between the synthetic receptor and the graphene surface to enable detection of biomarkers. The project aims to construct several linker chains consisting of polyaromatic units and these will be derivatized by *O*-alkylation. Additionally, graphene will be functionalized with the synthesized aromatic linker units. It will be investigated if the linkers bind to the graphene surface by non-covalent interactions. Lastly, two synthetic routes utilizing click-chemistry to produce a few triazole units were performed.

The focus of this Master's thesis project is specifically on the attachment of the biosensor on the graphene surface, hence the limitations of this project are the other investigated parts of the extensive project. Such limitations are the preparation of the synthetic receptor that can bind to biomarkers such as peptides and amino acids. Also, this project will not evaluate the binding ability of the biomolecules to the biosensor. Thus, detection of bacterial infections will neither be tested nor evaluated in this project. An additional limitation is whether the attached receptor can emit an electrical output on the graphene surface. In this project, certain polyaromatic units will be prepared, but there are also limitations on the different aromatic groups that will be investigated.

2
Background

To prepare the components of the biosensor, including a synthetic receptor and a polyaromatic linker chain, some organic reactions will be described in the following section. The theoretical background regarding the synthetic receptor will be described further as well as the reactions to produce the cyclized chains of triazole units including Sonogashira cross-coupling reactions and click-reactions. The aromatic linker will be prepared by *O*-alkylation via a nucleophilic substitution reaction. Furthermore, the graphene-coated chips will be functionalized with the aromatic compounds, hence the properties and the preparation of graphene will be described.

2.1 Biosensors and synthetic receptors

Biosensors are analytical devices used to detect the presence of a certain biomolecule, such as a protein, an amino acid or a peptide. The biosensor device consist of a sensing component that recognizes biomolecules from bacterial infections by selective binding; a signal transducer that produces a signal when a target molecule is encountered; and a reader device that monitors the signal [6]. Specifically in this project, a synthetic receptor is the sensing component.

Synthetic receptors are compounds whose structural and functional properties correspond to natural biosensors with recognition of biomolecules [2]. Hence, synthetic receptors imitate natural systems and can selectively bind to specific biomolecules such as peptides and amino acids. Molecular recognition is defined as the association of two or more molecules to the receptor via non-covalent interactions, including hydrogen bonds, van der Waals forces, metal coordination, and electrostatic-, hydrophobic- and π-π-interactions. The binding of amino acids and peptides origins from their specific properties and structures. For instance, amino acids and peptides can have side chains that are neutral, acidic, or basic, and these contribute to electrostatic charges, molecular polarity and hydrophobicity, which in turn result in certain interactions at the synthetic receptor. Also, the molecular structure of the biomarkers will determine the binding properties at the receptor, for instance for different stereoisomers, chiral recognition is of importance [5].

2.2 Triazoles and click-chemistry

In nature, biomolecules such as DNA, RNA, as well as some peptides, and vitamins contain nitrogen heterocycles, which is a class of compounds to which triazoles belong. Triazoles are five-membered heterocyclic compounds and can be either di- or trisubstituted by side groups R as shown in Figure 2.1. The compounds are of importance in many pharmaceutical applications due to their diverse properties. Hence, it is desirable to

produce triazoles by suitable synthetic methods, for instance by using click reactions [7]. Accordingly, the synthetic receptors consist of a cyclized chain of triazole units which is constructed by polymerization of triazole monomers. A single triazole is polymerized to form a dimer followed by a tetramer until a desired oligomer is obtained. Next, the ring is closed to form a cyclized chain called a macrocycle as shown in Figure 1.1 [8].

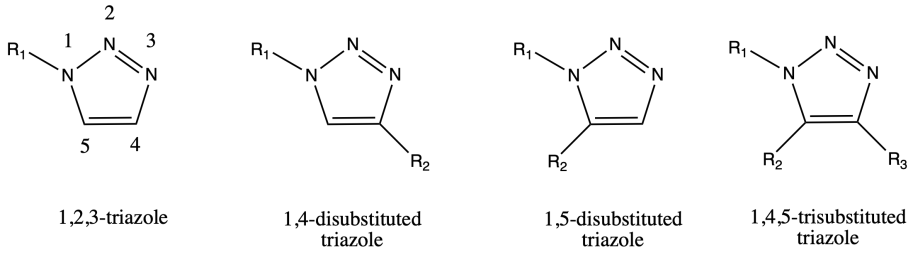

Figure 2.1: Four different triazoles including 1,2,3-triazole, 1,4- and 1,5-disubstituted triazoles and 1,4,5-trisubstituted triazole.

One established synthetic method to produce triazole monomers is the one-step click reaction between an alkyne and an organic azide. The click reaction is efficiently catalyzed by a copper (Cu) or ruthenium (Ru) complex to obtain different isomers, either the 1,2,3- or 1,2,4-isomeric triazole. By the copper-catalyzed azide alkyne cycloaddition (CuAAC) reaction, the 1,4 disubstituted 1,2,3-triazole is accessed. The ruthenium-catalyzed cycloaddition (RuAAC) provides the 1,5-disubstituted 1,2,3-triazole or the 1,4,5-trisubstituted triazole if internal alkynes are used [8]. Click reactions aim to link building units together and click chemistry is characterized by high stereospecificity and chemoselectivity as well as high efficiency in favorable conditions [9].

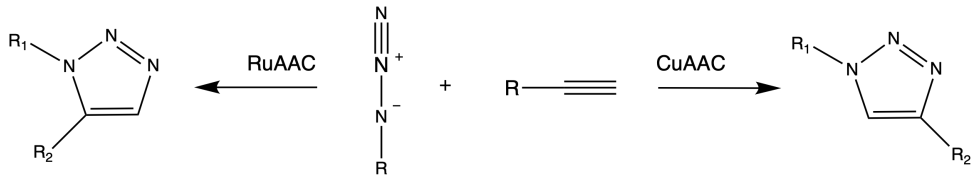

Figure 2.2: Catalyzed RuAAC and CuAAC reactions to produce 1,4- or 1,5-disubstituted triazoles.

2.3 The Sonogashira reaction

To produce triazoles, reactions between an azide and an alkyne are performed and the alkynes required in the click reactions can be prepared using the Sonogashira reaction. The Sonogashira coupling is a cross-coupling reaction using a palladium(0)-catalyst to form carbon-carbon bonds between a terminal alkyne and an aryl or vinyl halide. Addition of the co-catalyst copper(II)-iodide (CuI) supports the coupling of alkynes to organohalides. The reaction is performed under mild conditions such as at room temperature and in the presence of a base [10][11]. The general coupling reaction is presented in Figure 2.3 where R_1X is the aryl or vinyl halide. An example of how the preparation of arylated alkynes can be made is shown in Figure 2.4.

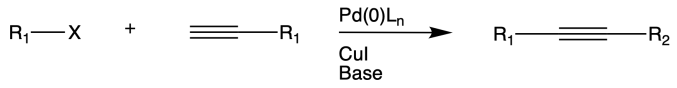

Figure 2.3: The general Sonogashira cross-coupling reaction.

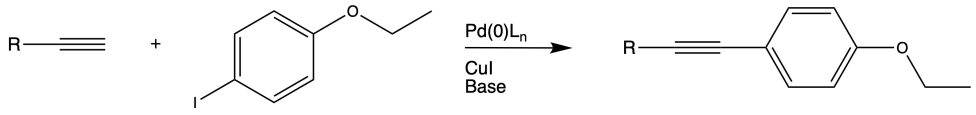

Figure 2.4: Derivatizing aromatic units via the Sonogashira coupling.

2.4 *O*-Alkylation of phenols

To attach the synthetic receptor to the graphene surface, a linker chain consisting of a polyaromatic hydrocarbon (PAH) system is the most suitable since it exhibits attraction to the graphene surface via non-covalent interactions [12]. Simple derivatized aromatic compounds can be prepared by using *O*-alkylation which is a nucleophilic substitution, where an alkyl chain substituent, R, is attached to the aromatic ring as in Figure 2.5. Further, the alkyl chain can be linked to the synthetic receptor [13]. In this project, polyaromatic groups of different size are investigated, including phenols with one aromatic ring and naphthols with two aromatic rings.

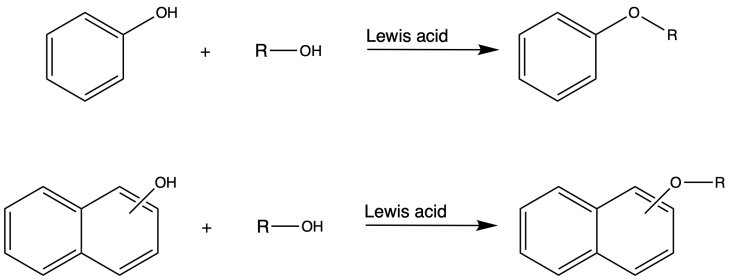

Figure 2.5: The general *O*-alkylation of phenol and naphthols via nucleophilic substitution.

The *O*-alkylation in this project is performed in the presence of a primary alcohol and a catalytic amount, either a Lewis or Brønsted acid [10]. A proposed mechanism is presented in Figure 2.6 for the alkylation of 2-naphthol. For this reaction, the aliphatic alcohol reacts with the Lewis acid, providing a proton which continues to react with the 2-naphthol to form a protonated carbocation. The aliphatic alcohol is a good nucleophile and attacks the carbocation while the leaving group, water, is displaced. This reaction is a direct nucleophilic substitution of the hydroxy group (OH). Consequently, the OH-group is the substituted element and water is the by-product in this reaction [14].

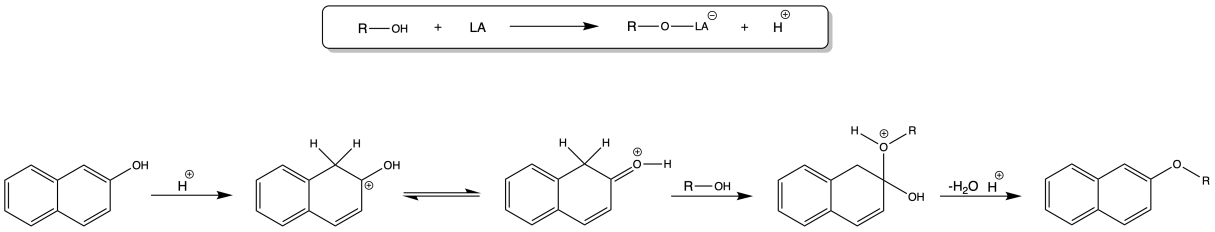

Figure 2.6: The proposed mechanism of *O*-alkylation.

2.5 Graphene

The synthetic receptor will be attached to a graphene surface via a polyaromatic linker chain. Graphene is an isolated two-dimensional (2D) monolayer of carbon atoms arranged in a hexagonal lattice structure. The carbon atoms are sp^2-hybridized and bind to each other via conjugated π-electrons [15]. The unique structure and physical characteristics of graphene generates special properties which are of interest in various technological fields. Among the properties of graphene are high electron conductivity, high mobility, thermal and mechanical stability, as well as large surface area [16] which make graphene a great material for biosensor applications. For this specific application, the advantage of graphene is the one-atom thick layer which provides a sensitive surface and is able to sense slight deviations in the surroundings. Hence, when an analyte in terms of the biomolecule bind to the synthetic receptor, the carbon atoms in the graphene will detect the variance of the conductivity and produce an electric output signal. The high sensitivity origins from the high electronic mobility - delocalized π-electrons moving more easily than in any other material. Due to the high sensitivity, very small amounts of analytes are required, thus the biosensing device has a low detection limit [2][17]. Accordingly, the peptide binding can be detected by sensing on the graphene surface through the polyaromatic unit [12].

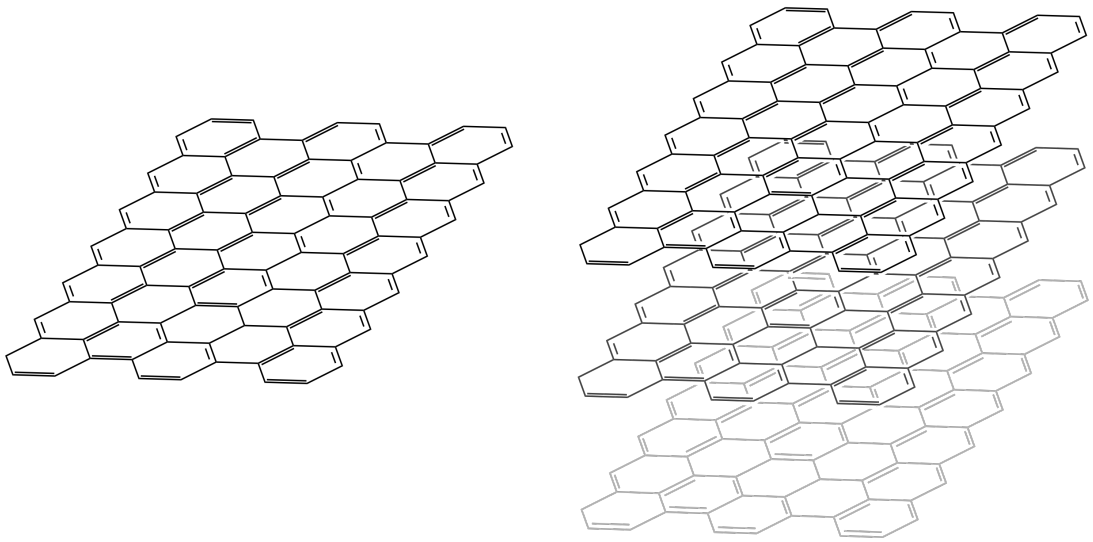

a) Graphene single-layer

b) Graphene multi-layer

Figure 2.7: One single-layer of graphene as a hexagonal lattice structure and multi-layer graphene sheets stacked on each other.

Layers of graphene sheets stack together by non-covalent π-π-interactions [16]. This also applies for stacking layers of polycyclic aromatic hydrocarbons; hence it is of interest to investigate the binding properties between the polyaromatic units and the graphene surface by π-π-interactions [18]. Generally, any molecule with aromatic rings can interact with graphene through π-π-stacking. A carefully studied PAH-compound for the biosensor application is 1-pyrenebutyric acid *N*-hydroxysuccinimide ester (PBASE) which consist of an aromatic pyrenyl group - a planar polycyclic segment with four aromatic rings in Figure 2.8 - that bind to graphene by non-covalent interactions [19]. A graphene surface functionalized with PBASE provides an efficient and stable link for sensing [17].

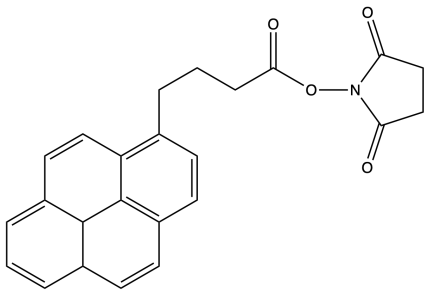

Figure 2.8: 1-Pyrenebutyric acid *N*-hydroxysuccinimide ester (PBASE).

In general, large polyaromatic units will contribute to a stronger interaction with the graphene surface due to a larger surface area, providing a better link. In this project, there is a risk that the prepared aromatic compounds might not have good interaction with the graphene surface depending on the number of aromatic rings. Compounds with few aromatic rings can have a weaker interaction; thus, it will not be suitable as a linker between the receptor and the graphene surface [12].

For the functionalization of graphene with the aromatic linkers, either covalent or non-covalent interactions can be implemented [20]. The advantage with non-covalent interactions are that they do not affect the properties or the structure of graphene, thus it retains the electronic conductivity [21]. In addition, the functionalization process with non-covalent interaction is simple because the linker can be physically adsorbed directly onto the graphene surface. The disadvantage of non-covalent interaction, however, is that the compounds may have poor stability, which could contribute to false signals in the mobility measurements. For covalent interactions, the compounds form chemical bonds to the carbon atoms in the graphene which provides a more stable environment and no uncertain signals. On the other hand, the covalent bonds are also more prone to damage the graphene structure [2].

Preparation of graphene can be done by chemical vapor deposition (CVD). The process of CVD is to produce a thin uniform film of solid material deposited over a substrate [15]. The desired material is exposed to an active environment inside a chamber, for instance heat, light and pressure, and becomes vaporized. Further, the vapor is deposited by chemical reaction on the surface [22]. For this project, the graphene is grown on a copper foil by low vacuum CVD. It is important that the copper substrate is free from oxides and other contaminations, thus the surface is cleaned with acetic acid before the CVD process. For the graphene growth, pre-diluted methane (5% CH_4 in argon) and hydrogen are added to the chamber which is heated to 950°C. When the graphene film is formed on

the copper substrate, PET is deposited on top of the graphene by using a laminator and glue, EVA which is a copolymer adhesive. The reason for using PET plastic for the chips is that it is an inexpensive, transparent and flexible material. It is desirable to have an affordable biosensor. Then, the copper is etched away with HNO_3 leaving a sample with graphene on top of a polymer chip [23]. The mobility of graphene can be measured by performing Hall-effect measurements which can be applied to materials that display the quantum Hall-effect (QHE) [24].

3
Results and Discussion

The aim of the project was to synthesize different aromatic linkers that potentially could bind to graphene via non-covalent interactions. In this section, the results of all reactions to produce the linkers will be presented. The linkers were to be attached to a graphene-coated chip by functionalization. Prior to the modification of the graphene surface, different solvents were tested to optimize the functionalizaton process. The results from the solvents experiments as well as the functionalization of graphene will be presented in this section. Additionally, some triazoles and also a triazole dimer were prepared as part of evaluating the click-reactions.

3.1 Synthesis of aromatic compounds by *O*-alkylation

Several aromatic compounds with an alkyl linker chain were prepared by utilizing O-alkylation of phenol and naphthol derivatives via nucleophilic substitution. The reactions were performed in the presence of a linear primary alcohol and a catalytic amount of a Lewis acid. For this reaction presented in Figure 3.1, 1-propanol, and boron trifluoride ($BF_3 \cdot OEt_2$) were selected. Initially, a series of phenols, with one aromatic ring, were investigated. Two halogen substituted phenols were examined because they could possibly be attached to another compound further on, for example the synthetic receptor. The reactions were performed to obtain compounds **1**, **2** and **3**. However, the desired products were not formed using this experimental method and it is possible that the phenols were not nucleophilic enough resulting in a very low reactivity. These compounds can be produced by utilizing an alternative reaction route with alkyl halides. However, those reactants are toxic and cancerogenic, so for this project it was desired to implement green chemistry by using environmentally friendly chemicals.

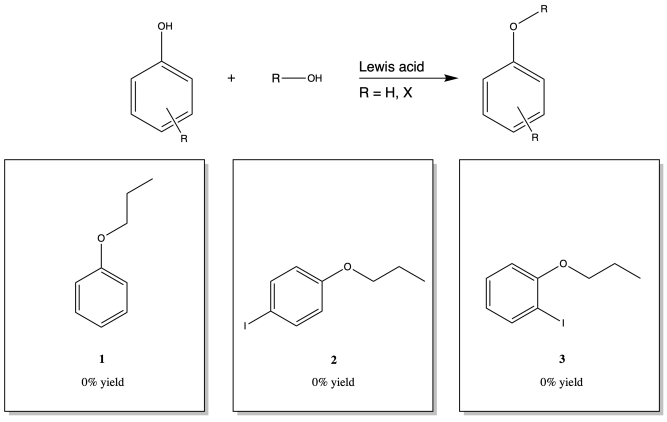

Figure 3.1: The general *O*-alkylation reaction scheme of phenols to produce three different aromatic compounds **1-3**.

The experiments proceeded by investigating a series of naphthols, with two aromatic rings, that were mono- or disubstituted by hydroxyl groups. The same method was utilized to obtain the compounds **4-8** as shown in Figure 3.2.

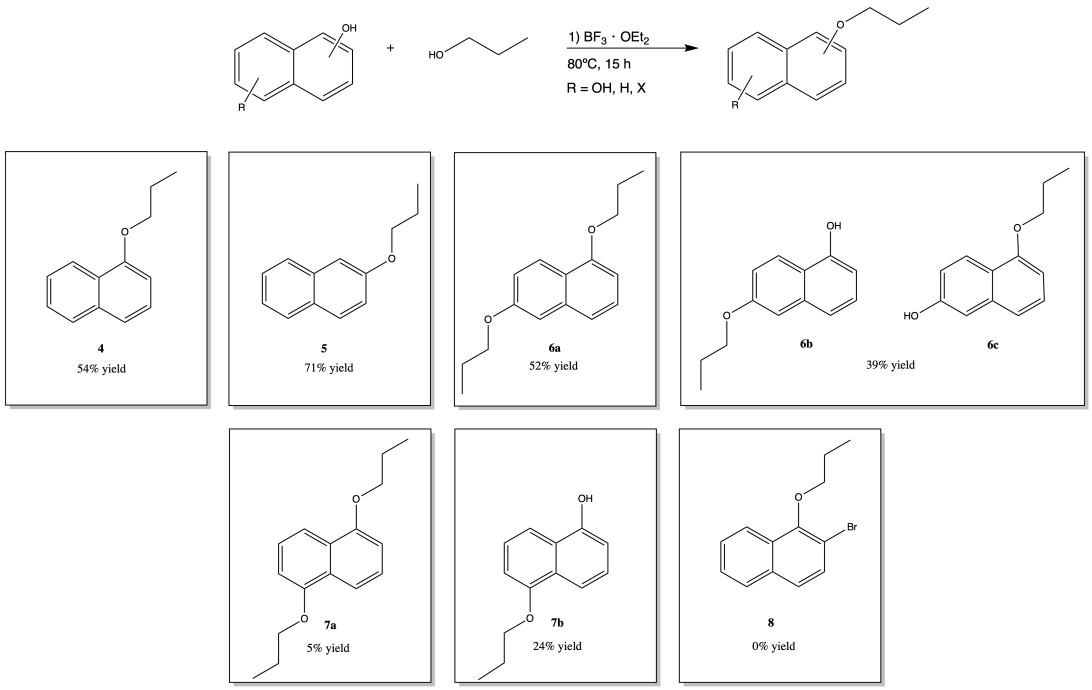

Figure 3.2: The general *O*-alkylation reaction scheme of naphthols to prepare the aromatic compounds **4-8**.

The formation of 1-propoxynaphthalene **4** had a yield of 54% while the synthesis of 2-propoxynaphthalene **5** had a higher yield of 71 %. When comparing the conversion of **4** and **5** considering the starting materials 2-naphthol and 1-naphthol, it is supposed that the 2-naphthol has a higher reactivity to form the carbocation due to a higher mesomeric effect than the 1-naphthol. Moreover, the higher reactivity of the 2-naphthol originates from the higher electronic charge density at the first carbon in 2-naphthol compared to the second carbon in the 1-naphtol [14].

For a broader scope of investigation, dihydroxynaphthalenes were studied to obtain the compounds **6a**, **6b**, **6c**, **7a** and **7b**. In the reaction of 1,6-dihydroxynaphthalene **6a**, also monosubstituted products were obtained as a mixture of 6-propoxynaphthalene-1-ol **6b** and 5-propoxynaphthalene-2-ol **6c**. The yields obtained were 52% of **6a** and 39% of **6b** and **6c**. The formation of 1,5-dihydroxynaphthalene **7a** had a low yield of 5% while the monosubstituted 5-propoxynaphthalene-1-ol **7b** was the major product formed in this reaction, but still with a low yield of 24%. The higher formation of **6a** in comparison to **7a** can also be explained by the proposed suggestion that 2-naphthols have a higher reactivity than the 1-naphthol derivatives due to the electronic charge densities.

Additionally, one reaction using a halogenated naphthol was performed to obtain 2-bromo-1-propoxynaphthalene **8** but the product was not detected. Perhaps, there was no conversion due to a low reactivity caused by the electronic effect.

Moreover, all reactions were performed only once, consequently, the results could be affected by the human source of error and the reaction conditions including choice of Lewis

acids, reaction time and temperature. To optimize the reactions for a desired product and full conversion of the starting material, they should be repeated several times and the conditions should perhaps be changed.

3.2 Synthesis of aromatic compounds by *N*-arylation

The last aromatic reaction performed was to produce *N*-propylaniline **9** containing a nitrogen instead of oxygen because it was of interest to investigate how it would affect the interaction with graphene and then compare it with the *O*-alkylated compounds. For this reaction, another method was implemented by using *N*-arylation shown in Figure 3.3.

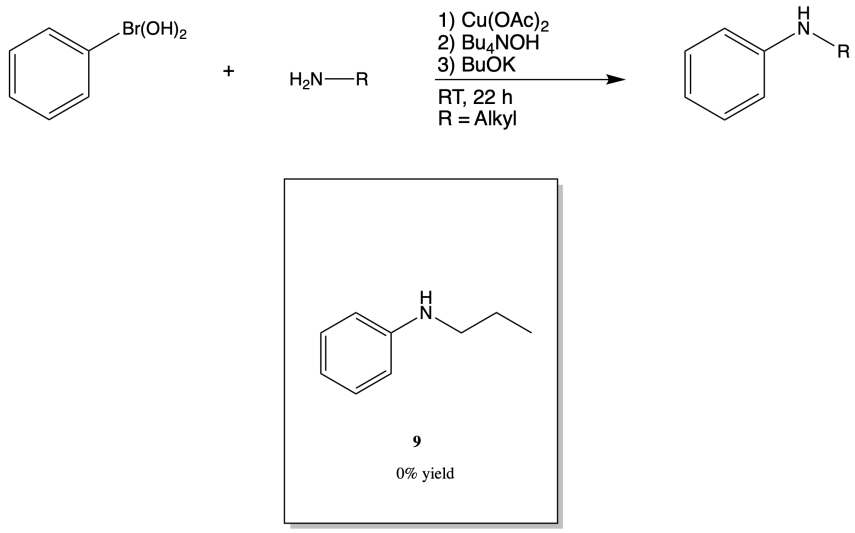

Figure 3.3: The general *N*-arylation reaction scheme to prepare the aromatic unit **9**.

Propylamine was reacted with phenylboronic acid and BuOK, and the reaction was catalyzed by copper acetate in 40% aqueous solution of Bu_4NOH and stirred at room temperature overnight. The product **9** was not obtained however. Presumably, the reaction did not work because an acid, HCl, was added during the extraction which could have protonated the product, so it ended up in the water phase and was lost. Another possible reason why the reaction did not work is that one of the reagents was no longer reactive.

3.3 Synthesis of triazoles

A few triazoles were prepared using click-chemistry, either via CuAAC or RuAAC reactions. The ambition was to ultimately attach one of the synthesized triazoles to a selected aromatic linker which had been prepared in previous experiments.

For the formation of the first triazole **10** in Figure 3.4, the reaction was performed under nitrogen atmosphere and in the presence of ruthenium-catalyst [$Cp^*RuCl(COD)$] which was dissolved in DCM. Then propargyl alcohol followed by benzyl azide were added to the reaction mixture that was allowed to stir at room temperature overnight. The desired product **10** was not obtained however since no conversion was observed. The reaction was performed twice because the first time, benzyl azide was added prior to the propargyl

alcohol which could have deactivated the catalyst. Despite adding the compounds in different order the second time, the reaction did not work.

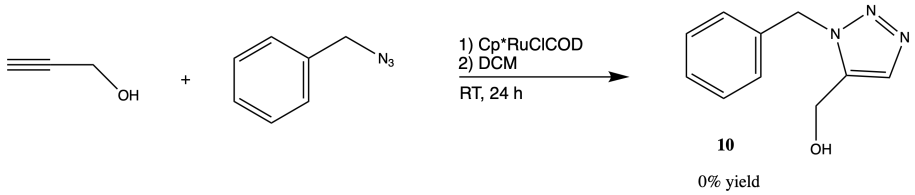

Figure 3.4: Preparation of the triazole **10** via the catalyzed RuAAC reaction.

To produce the second triazole **11** shown in Figure 3.5, the reaction was performed under a nitrogen atmosphere and in the presence of the copper-catalyst, copper(II)sulfate, and the reducing agent, sodium ascorbate. The solvent used was a mixture of water and the alcohol *tert*-butanol in a ratio of 1:1 to solubilize the substrates. After addition of propargyl alcohol and methyl azidoacetate, the reaction was stirred at room temperature overnight. As a result, the product was obtained since it could be observed in the ^{1}H NMR spectrum. However, the product contained a lot of water, which could also be observed in the ^{1}H NMR spectrum, hence the yield could not be calculated.

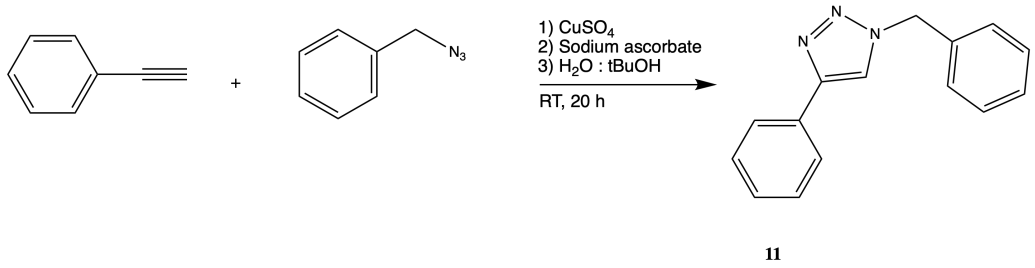

Figure 3.5: Preparation of the triazole **11** via the catalyzed CuAAC reaction.

A substrate commonly used for interaction with graphene is called PBASE **12** and the compound is commercially supplied. Since PBASE has formerly been used for graphene modification within biosensing application [25][17], it was interesting to further analyze the compound for this purpose. The aim was to attach a simple triazole to the PBASE as shown in Figure 3.6, to obtain a simple synthetic receptor. The four aromatic rings would enable interaction with graphene and the the triazole would interact with biomolecules.

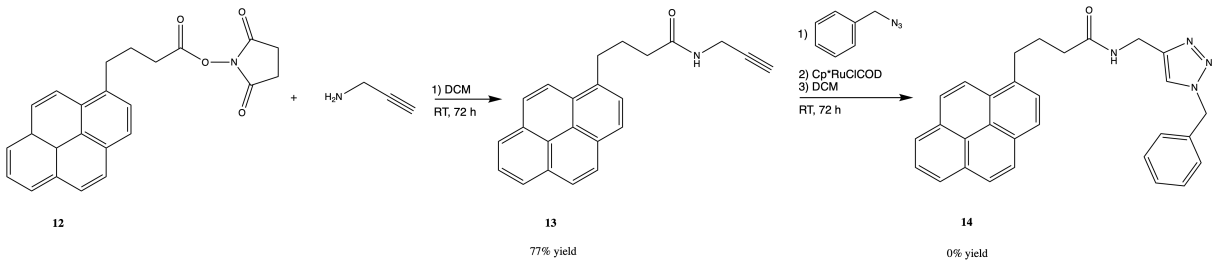

Figure 3.6: Preparation of the alkyne **13** via Sonogashira reaction and further reaction to produce the triazole **14** via the catalyzed RuAAC reaction.

The first step was to produce the alkyne **13** by reacting PBASE with propargyl amine in solution with DCM. The reaction was stirred at room temperature during three days for

formation of **13** and a yield of 77% was obtained. Next, it was desired to produce the triazole **14** and two methods were implemented. The same methods utilized for compounds **11** and **10** were applied but no product was obtained in neither of the attempts. It is assumed that the reaction conditions must be optimized in order to obtain the desired product. An option could be to prepare a triazole separately and then attach it to **13**.

3.4 Synthesis of a triazole dimer

To produce a dimer, a certain reaction route was followed starting with preparing an alkyne. For the formation of the alkyne **15**, a solution of *N*-Boc-propargylamine, iodobenzene and copper(I)-iodide in dry acetonitrile was prepared and the reaction was catalyzed by a palladium complex under nitrogen atmosphere. Triethylamine was added and the reaction was stirred at room temperature overnight to obtain a yield of 94% of compound **15**. In the following reaction, the alkyne was used for the synthesis of triazole **16a** via the catalyzed RuAAC reaction. The ruthenium catalyst was dissolved in DCM under nitrogen atmosphere followed by addition of the alkyne and methyl azidoacetate. The reaction was performed twice and the first time, a mixture of the two triazole isomers were obtained, 67% yield of the first isomer **16a** and 14% of the second isomer **16b**, which could be confirmed in the ^{1}H NMR spectrum. Later, it could be distinguished which isomer was which by studying 2D NOESY NMR to obtain stereochemical information. This was done by supervisor Flavia Ferrara. The second time, the isomers were not completely separated so only a fraction of the first isomer **16a** could be isolated with a yield of 52% and was used further.

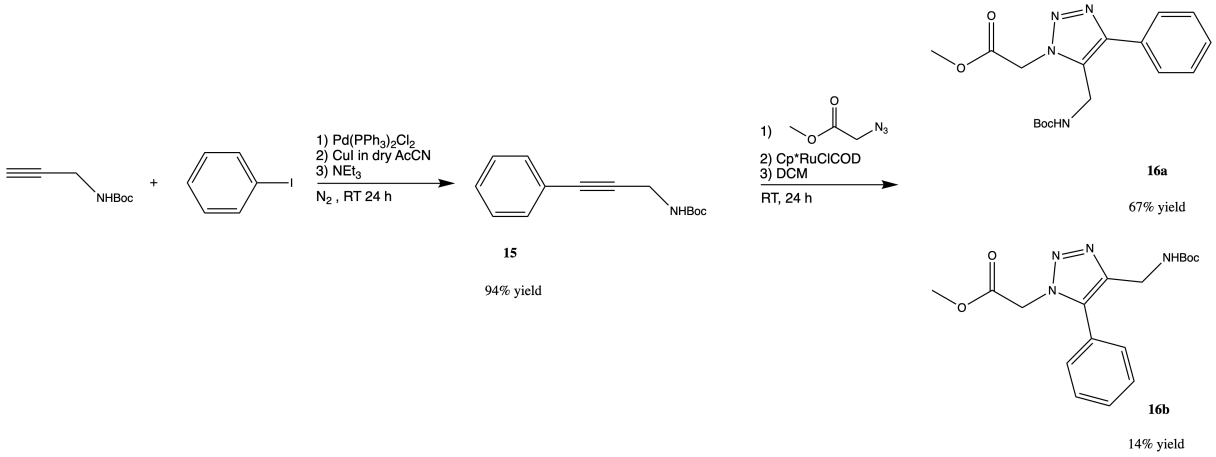

Figure 3.7: Synthetic route for producing an alkyne **16** via Sonagashira followed by formation of two triazole isomers **16a** and **16b** via catalyzed RuAAC reaction.

Next, deprotection of the Boc-group was made on the first isomer **16a** in solution of DCM and THF to obtain the Boc-deprotected product **17** in Figure 3.8. The second isomer **16b** was used for ester hydrolysis to transform the ester to a carboxylic acid **18**. The isomer was dissolved in Me-THF and NaOH was added. Then the reaction mixture was put into a microwave for 15 minutes at 100 °C. However, this reaction did not work, which affected the following dimer synthesis. Another method was tried and therefore the triazoles had to be reproduced. As mentioned earlier, only the first isomer **16a** could be isolated and this was used for the new ester hydrolysis method to produce **19**. For this reaction, the

triazole isomer was dissolved in methanol reacted with LiOH to form a carboxylic acid. This method worked because the dimer **20** was formed in the following reaction which could be confirmed by ^{1}H NMR. Compound **17** and **19** were reacted in a solution of DCM and in the presence of HATU and DIPEA. As a result, the dimer was obtained with a yield of 5%. By repeating the reaction and possibly by optimizing the reaction conditions, a higher yield can most likely be obtained. Perhaps by using dimethylformamide (DMF) in a ratio of 1:1 (DMF:DCM) together with HATU and DIPEA could increase the yield.

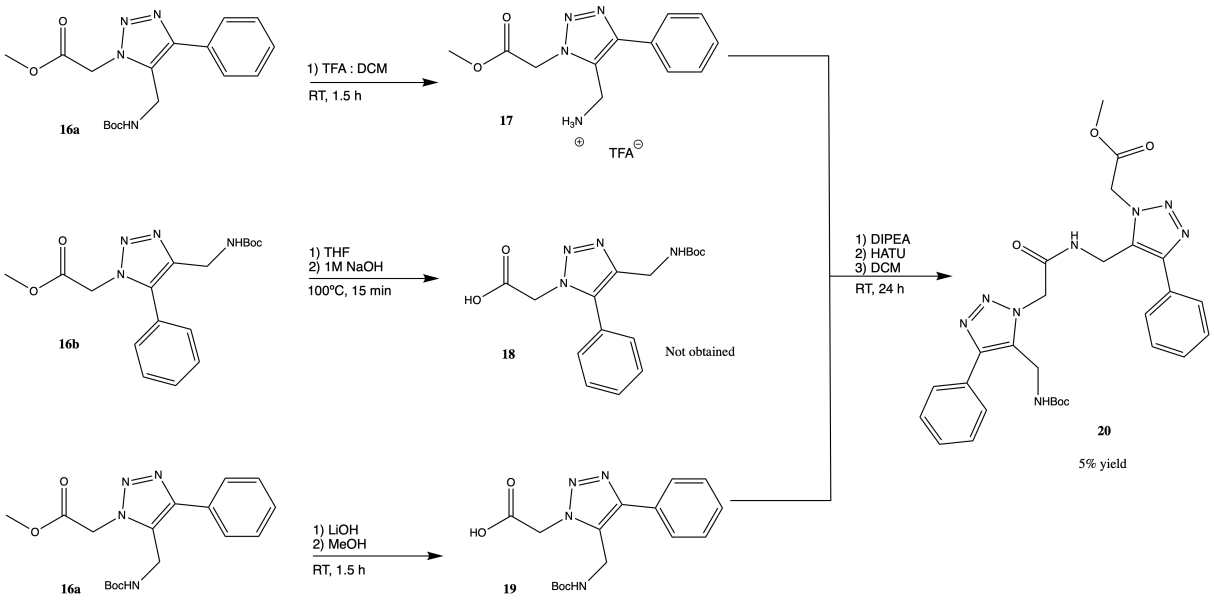

Figure 3.8: Synthetic route to produce the dimer **20** via deprotection of the Boc-group **17** and ester hydrolysis of **16a** to **19**.

3.5 Solvent effect on graphene

The next experimental part was to examine if the obtained aromatic compounds **4, 5, 6a, 6b, 6c, 7a, 7b** bind to the graphene via non-covalent interactions. The compounds were to be dissolved in a selected solvent to enable the dissolution of the compounds on the graphene surface. Accordingly, to prepare for the functionalization of graphene, some solvents were investigated to optimize the conditions in order to improve the final experiments. It was important that the solvents were compatible with the EVA/PET chips as well as the graphene and should not dissolve or damage the chips. Also, the solvents should not change the mobility of graphene since it should only be affected when something is binding to the surface, for example the aromatic compounds, the receptors and the biomarkers. Hence, different solvents were tested to see which could be suitable and compatible with the EVA/PET and graphene samples.

In the first test, seven different solvents were tested as presented in Table 3.1. The control samples were left as a reference and were therefore not treated with the solvents. From the results, it could be concluded that DCM and tetrahydrofuran were incompatible with PET because the chips were damaged after being exposed to these two solvents for two hours. It is mainly the PET that has low resistance to the solvents and gets dissolved. The other solvents displayed higher compatibility and could be tested in further experiments.

It is expected that the mobility changes or differs slightly between measurements, as seen for the control samples, because the Hall-effect measurements are inevitably performed on different sites of the graphene samples each time. In all three experiments, it could be observed that the five other solvents affected the mobility a lot when comparing the measured mobilities prior to and after the experiment in Table 3.1. Thus, it was convenient to understand why this was happening and what could be done to prevent the deviations of the mobility. It was assumed that the solvents were not evaporated completely because they got trapped between the multi-layer patches of graphene. During the growth of graphene by CVD, perhaps an uneven distribution of layers were formed, resulting in two or more layers of graphene. This contributed to intercalation of the solvents and the amount of solvent trapped under the multi-layers differed for different samples. Hence, the solvents affected the mobility of graphene to different degrees. Therefore, the samples were kept in nitrogen gas overnight in an attempt to evaporate some solvent as shown in Table 3.1. As a result, the mobility of the graphene samples changed and returned closer to the original value, but it was still a big difference.

Table 3.1: Mobility ($cm^2V^{-1}s^{-1}$) measured by Hall-effect measurements prior to and after graphene chips were treated in different solvents for two hours. The mobility was also measured after exposed to N_2 gas overnight.

Test 1				
Vial	**Solvent**	**Mobility before**	**Mobility after**	**Mobility after N_2**
1	Control	1296	1199	1470
2	Diethyl ether	3677	11270	3555
3	DCM	3968	Damaged	Damaged
4	Ethanol	2980	4888	4750
5	1,4 dioxane	4089	4501	4303
6	THF	2964	Damaged	Damaged
7	Acetone	7165	5167	8928
8	EtOAc	3883	4258	4479
9	Control	2466	2880	2866
Test 2				
Vial	**Solvent**	**Mobility before**	**Mobility after**	**Mobility after N_2**
1	Diethyl ether	4444	6812	5322
2	Control	2460	2891	3095
3	Ethanol	7940	Damaged	Damaged
4	1,4 dioxane	7796	28980	Damaged
5	Acetone	7178	8321	8454
6	EtOAc	4264	5518	5105
Test 3				
Vial	**Solvent**	**Mobility before**	**Mobility after**	**Mobility after N_2**
1	Control	2420	2730	2670
2	Diethyl ether	3990	584	2970
3	Ethanol	3410	1120	4840
4	1,4 dioxane	2630	4070	3830
5	Acetone	1220	758	2890
6	EtOAc	1590	3830	5105

The reason for performing these experiments was to optimize the process and to have more reliable results in the functionalization experiments. Therefore, one solvent was selected in a fourth test to be more consistent and the solvent effect on mobility was investigated. Diethyl ether was selected since it was compatible with the graphene samples and dissolved most of the aromatic compounds. This time, the remaining solvent was evaporated by keeping the samples in a chamber at 60 °C and in constant flow of nitrogen overnight.

Table 3.2: Mobility ($cm^2V^{-1}s^{-1}$) measured by Hall-effect measurements prior to and after graphene chips were treated in diethyl ether for two hours. The mobility was also measured after exposed to N_2 gas overnight and at 60 °C overnight.

Test 4				
Vial	**Mobility before**	**Mobility after**	**Mobility after N_2**	**Mobility 60°C**
1	2760	-2080	-815	3000
2	3000	-914	246	3020
3	2240	-1890	-979	2080
4	2190	-2080	-769	2650
5	3520	-3940	-2170	3710
C	4080	4340	4210	4430

After treatment with diethyl ether, it appeared that the graphene samples had been electron doped because the measured mobility after the experiment had negative values. After keeping the sample in N_2 overnight, some of the trapped solvent evaporated, so the mobility recovered to some extent. However, some amount of solvent was still trapped resulting in either negative mobility values or low mobility. After keeping the samples at 60 °C under constant flow of N_2 overnight, the mobilities recovered to the original values and it could be assumed that all solvent was removed completely.

Another factor that could affect the change in mobility to some extent is contaminations that could be trapped between the PET and the graphene layer. The contaminations could have appeared from the CVD process even though the substrates were cleaned. Therefore, it is uncertain as to whether the mobility measurements are affected by both solvent and contaminations.

3.6 Attachment of the linker to graphene

With knowledge from the solvent experiments, a better method was developed and could now be implemented in the experiments of attaching the aromatic compound to the graphene surface. The synthesized compounds, **4**, **5**, **6a**, **6b**, **6c**, **7a**, **7b** presented in Figure 3.2 and two commercially supplied compounds, PBASE **12** and 1-pyrenecarboxaldehyde **21** in Figure 3.9 were tested in the experiments. The compounds were dissolved in diethyl ether at a concentration of 5 mM and the graphene samples were incubated in each compound for two hours at room temperature. The mobility of the graphene samples was measured prior to and after the experiments.

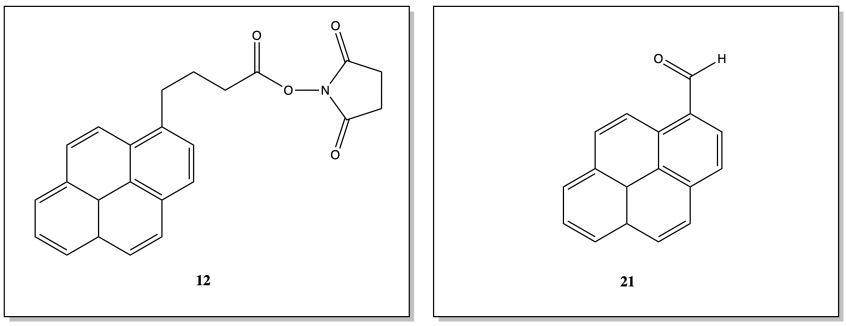

Figure 3.9: Commercially supplied compounds **12** and **21** which were used for functionalizing of graphene.

The purpose of the experiments was to examine if the aromatic linker interacted with graphene and attached to its surface by non-covalent bonds. By measuring the change of mobility, it could indicate if something is on the surface. A slight change in mobility is expected since the measurement points will differ for each measurement, as is observed for the control samples. The fluctuation of mobility should also be considered for all graphene samples which were functionalized. Hypothetically, it is expected that when a compound binds to the graphene surface, the mobility will decrease because the compound contributes to a resistance for the electron to move over the graphene surface.

Table 3.3: Mobility ($cm^2V^{-1}s^{-1}$) measured by Hall-effect measurements prior to and after graphene samples were functionalized with seven different compounds for two hours. Graphene samples were rinsed with clean solvent after functionalization.

Test 1			
Vial	**Compound**	**Mobility before**	**Mobility after N_2 and 60 °C**
1	**4**	4030	4400
2	**5**	3180	3710
3	**7b**	2940	3990
4	**7a**	3630	3680
5	**6a**	3540	4060
6	**6b, 6c**	3330	2400
7	**21**	1440	1600
8	Control	940	1390

From the results in the first experiment, it is observed that the mobility for most compounds returned to the original mobility after the functionalization as presented in Table 3.3. The compounds that showed a decrease in mobility were the mono-substituted naphthols **6b** and **6c**, which could indicate that the compounds have attached to the surface of graphene. Regarding the other compounds which did not affect the mobility significantly, it is possible that they did not interact with the graphene but were washed off when rinsing the samples with clean solvent to remove excess compound.

Table 3.4: Mobility ($cm^2V^{-1}s^{-1}$) measured by Hall-effect measurements prior to and after graphene samples were functionalized with seven different compounds for two hours. Graphene samples were not rinsed with clean solvent after functionalization.

Test 2			
Vial	**Compound**	**Mobility before**	**Mobility after N_2 and 60 °C**
1	**4**	2070	Damaged
2	**5**	5110	4590
3	**7b**	5620	4830
4	**6a**	5780	5350
5	**6b, 6c**	2400	2180
6	**12**	4400	2380
7	**21**	4980	4920
8	Control	3290	3400

A second experiment was performed without washing the the samples with clean solvent after the functionalization. Damaged samples are most often due to handling the chips with the tweezers. From the results, it could be observed that compounds **7b** and **12** had a significantly lower mobility, which could indicate that the compounds attached to the graphene surface. However, it could not be excluded that the compounds solely are present on top of the surface without interaction. Hence, this method is not enough for establishing if the compounds are on the surface or not. In order to confirm if the compounds have bound to the graphene, it is convenient to utilize other characterization techniques.

Table 3.5: Mobility ($cm^2V^{-1}s^{-1}$) measured by Hall-effect measurements prior to and after graphene samples were functionalized with six different compounds for two hours. Graphene samples were not rinsed with clean solvent after functionalization.

Test 3			
Vial	**Compound**	**Mobility before**	**Mobility after N_2 and 60 °C**
1	**4**	5270	3620
2	**5**	6590	3790
3	**7b**	5500	3320
4	**6a**	3470	2580
5	**6b, 6c**	3060	Damaged
6	**12**	4420	3240
7	Control	4840	5160

To gain more understanding of the interaction between the compounds and the graphene, Raman spectroscopy was performed prior to and after the functionalization in the third experiment. Also, no rinsing with clean solvent was performed. It was observed that most compounds resulted in a lower mobility which could indicate that the compounds had interacted with graphene, however, it is not possible to know if the mobility also changes because the compounds are laying on top of the graphene surface. When studying the Raman spectra as presented in Appendix B, no new peaks appeared for compounds **4**, **5**, and **6a**. The existing peaks in their spectra are from PET/EVA on graphene which could be confirmed by Munis Khan at MC2. If the peaks of the compounds were in the same range as the PET/EVA, they would therefore not be visible.

Interpreting the results of Raman spectra for compounds **7b**, **6b**, **6c** and **12**, new peaks appeared after the functionalization which could be signals from the linkers. For the mono-substituted compounds **7b**, **6b** and **6c**, a broad peak is present from 1700 to 2600 cm^{-1} which could perhaps be from the hydroxy group. For PBASE **12**, the visible peak at 1400 cm^{-1} is similar to literature results, so it is most likely an indication that PBASE bind to graphene [17]. However, it is not evident if the compounds have formed non-covalent bonds to the surface or if they are laying on top.

Table 3.6: Mobility ($cm^2V^{-1}s^{-1}$) measured by Hall-effect measurements prior to and after graphene samples were functionalized with six different compounds for two hours. Graphene samples were rinsed with clean solvent after functionalization.

Test 4			
Vial	**Compound**	**Mobility before**	**Mobility after N_2 and 60 °C**
1	**4**	1420	1390
2	**5**	4050	3290
3	**7b**	4720	3120
4	**6a**	4860	4370
5	**6b, 6c**	3760	1900
6	**12**	3020	Damaged
7	Control	5700	5210

In the fourth experiment, the samples were washed with clean solvent after functionalization to exclude the possibility that the compounds are present on the surface. Once again, Raman measurements were made and the observed results were similar to the results in the third experiments. For compound **4**, **5**, and **6a** no new peaks appeared and also no significant changes in the mobility were observed. Hence, it is most likely that these compounds do not bind to graphene. For compounds **7b**, **6b**, **6c** and **12**, new peaks appeared again. When comparing the Raman spectra from the third and the fourth experiment, the peaks for the same compounds looked different, and this could be due to the clean washing of the samples. Additionally, the mobilities for compounds **7b**, **6b**, **6c** and **12** were decreased. The results from both Raman and mobility measurements are an indication that the compounds interacted with the graphene, but further investigation is required to confirm it.

Furthermore, it is of importance that the compounds dissolve well in the solvent in order to properly distribute the compounds on the graphene surface. It was difficult to dissolve PBASE **12** due to its larger size and this could affect the ability for the compound to interact with graphene. As mentioned before, PBASE has been used for biosensing applications by modification of graphene and this compound is assumed to be the most promising. In general, from this experiment, is not possible to distinguish if the compounds bind to graphene or not by utilizing this method. Multiple experiments should be performed while also varying functionalization time, concentration, solvent and characterization techniques for example Mass Spectroscopy (MS) and X-ray Photoelectron Spectroscopy (XPS).

3.7 Future studies

For future studies it would be interesting to synthesize a series of PAH-compounds with varying size, from two to several aromatic rings. It is assumed that larger linkers consisting of four or more aromatic rings, will have a stronger and more stable non-covalent interaction with graphene due to the larger surface area. For instance, tricyclic anthracenes and pyrenes with four aromatic rings such as PBASE are some options which could be investigated further. It would also be interesting to compare several aromatic compounds with both oxygen- and nitrogen-substituted alkyl chains and examine how the substituted atom will affect the interaction with graphene. In addition, a more complex polyaromatic group can be prepared using transition metal-catalyzed cyclotrimerization.

For the functionalization of graphene, another method could possibly be implemented. Sublimation of the compound over the surface is an alternative way of distributing the compounds on the graphene instead of using solvent. This would avoid several drawbacks such as difficulties in dissolving larger compounds in a suitable solvent, and also having solvent stuck in the multi-layers of graphene, affecting the mobility. Another aspect to consider is if the linker compounds are stable enough to be vaporized without degrading. Not only do the aromatic chains need to be stable, but also the synthetic receptor that eventually is obtained and connected to the linker. It would require more knowledge about the compounds before this method could be established.

The ambition was to ultimately attach one of the synthesized triazole units to a selected poly-aromatic compound through the alkyl linker chain which had been prepared in previous experiments. Thus, such a product consisting of both the aromatic compound and a single triazole unit would resemble a simplified synthetic receptor that could be further investigated in the graphene experiments. It would be interesting to see how the triazole unit would affect the mobility of graphene and also if the Raman measurements would show more distinct peaks. At last, it requires further studies to produce a complete synthetic biosensor which consists of a PAH-system such as PBASE and a cyclized chain of triazole units, perhaps a tetramer. It would also be convenient to investigate the geometry of the complete molecule since it could affect the interaction to graphene depending on if it is planar to the surface or not. Further, it would be interesting to investigate if the compound binds to graphene via non-covalent interactions.

4
Conclusion

In this Master's thesis, the linking of synthetic receptors to a graphene surface for biosensor applications was investigated and evaluated. Synthesis of polycyclic aromatic hydrocarbons (PAH) linker chains by *O*-alkylation was performed. Initially, simple aromatic compounds including phenols and naphthols, were alkylated with a propyl group. As a result, several aromatic linker chains derived from mono- and di-substituted naphthols were obtained successfully with the selected synthesis method, while no alkylated phenols were obtained.

Furthermore, the derivatized aromatic compounds as well as two commercially supplied pyrenes, with four aromatic rings, were functionalized on a graphene-coated EVA/PET chip. Then, the binding of the compounds to the graphene surface via non-covalent interactions was investigated. The experiments were performed using Hall-effect measurements to observe the electron mobility of the graphene and how it changed after functionalization. Also, Raman spectroscopy was implemented to examine if the polyaromatic compounds had attached to the graphene surface. However, it could not be confirmed if the linkers had interacted with the graphene but the results showed an indication that some of the compounds did interact. Consequently, it was not possible to evaluate the non-covalent interactions from the obtained results. PBASE is the most promising compound in this project and it has also been used to modify graphene in previous studies.

In addition, further experiments are required and what should be considered is that PAH-compounds with more aromatic units such as anthracenes and pyrenes have a stronger and more stable non-covalent interactions with graphene due to a larger surface area. Also, additional characterization techniques could be used to analyze the functionalized graphene surface, for instance Mass Spectroscopy (MS) and X-ray Photoelectron Spectroscopy (XPS).

Synthetic reactions utilizing click-chemistry to produce triazoles and one triazole dimer were performed. The triazoles and the dimer were synthesized successfully, however, the reactions could be optimized further to obtain higher yields. Moreover, a goal was to attach one of the triazole units to a synthesized polyaromatic compound through the alkyl linker chain, for instance the PBASE-linker. This product was never obtained but it is of interest to continue with this in future studies. The product would resemble a simplified synthetic receptor that could be studied in the graphene experiments.

5

Experimental procedures

The polyaromatic linker chain units between the synthetic receptor and the graphene chip were synthesized and the selected experimental method *O*-alkylation is described in this section. The compounds were then functionalized on a graphene surface and the interaction between the linker chain and graphene was examined. Also, the procedures for synthesizing single triazole units and a triazole dimer are described in this section including Sonogashira coupling to produce arylated alkynes followed by click-reactions.

5.1 General methods

All reactions were conducted using magnetic stirring in either air or dry nitrogen atmosphere. All reagents used were commercially supplied and no further purification was made. Thin layer chromatography (TLC) was performed on aluminum foils coated with silica gel (0.20 mm, 254 nm) and visualized under ultraviolet light (ν = 365 nm). Separations using Biotage Isolera Flash column chromatography were performed on Biotage Sfär Silica D 60 µm. ^{1}H NMR spectra were obtained utilizing the instrument VARIAN 400 at 400 MHz in $CDCl_3$ and the reference peak of $CDCl_3$ was set to 7.26 ppm. The graphene PET/EVA chips were provided from a collaborate researcher, Munis Khan, at the MC2 department. The graphene was grown on 25 µm copper foil by low vacuum chemical vapor deposition (CVD) at a maintained pressure of 70 mBar. The graphene was transferred to EVA/PET chips (1 cm x 1 cm) by hot lamination and the copper was etched with HNO_3.

5.2 Preparation of aromatic linkers by *O*-alkylation

Eight different aromatic compounds were synthesized according to the general procedure and the reaction schemes of propoxybenzene **1**, 1-iodo-4-propoxybenzene **2**, 1-iodo-2-propoxybenzene **3**, 1-propoxynaphthalene **4**, 1-propoxynaphthalene **5**, 1,6-dipropoxynaphthalene **6a**, 1,5-dipropoxynaphthalene **7a** and 2-bromo-1-propoxynaphthalene **8**, are presented in Table 5.1.

General procedure: To a 10 mL tube, the aromatic compound (1 mmol), propanol (10 mmol, 0.75 mL) and boron trifluoride (1.2 mmol, 0.3 mL) were added. The tube was sealed and the reaction mixture was allowed to stir at 80°C for 15 hours. To indicate if the product was obtained, TLC was performed on the crude product (petroleum ether : ethyl acetate = 9:1). Further, the organic reaction mixture was transferred to a separatory funnel, quenched with distilled water (10 mL) and extracted with DCM (3 x 10 mL) three times. The organic phase was collected and washed with brine (10 mL) and then dried with sodium sulfate. At last, the crude product was filtrated and the solvent was evaporated.

To isolate and purify the product, flash column chromatography was performed with a gradient of 0 to 10% ethyl acetate in petroleum ether. Further, ^{1}H NMR was used to analyze the product and control if the desired product was obtained.

Table 5.1: *O*-alkylation reactions performed with the aromatic units, 1-propanol and boron trifluoride ($BF_3 \cdot OEt_2$) at 80°C for 15 hours.

Reaction	Reaction scheme
1	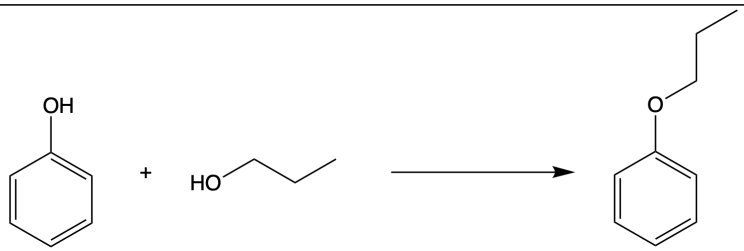 **1** 0% yield
2	 **2** 0% yield
3	 **3** 0% yield
4	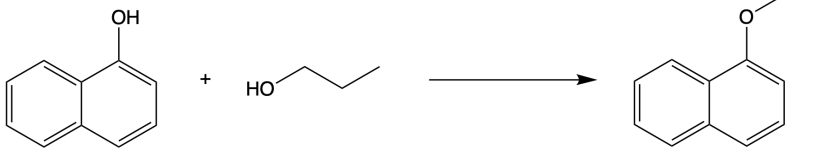 **4** 54% yield
5	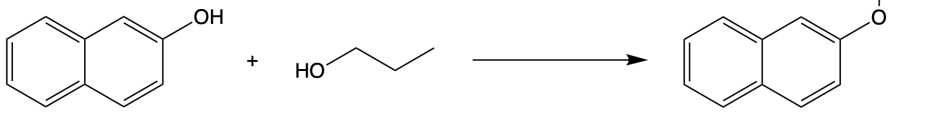 **5** 71% yield

Continued on next page

Table 5.1 – continued from previous page

Reaction	Reaction scheme
6	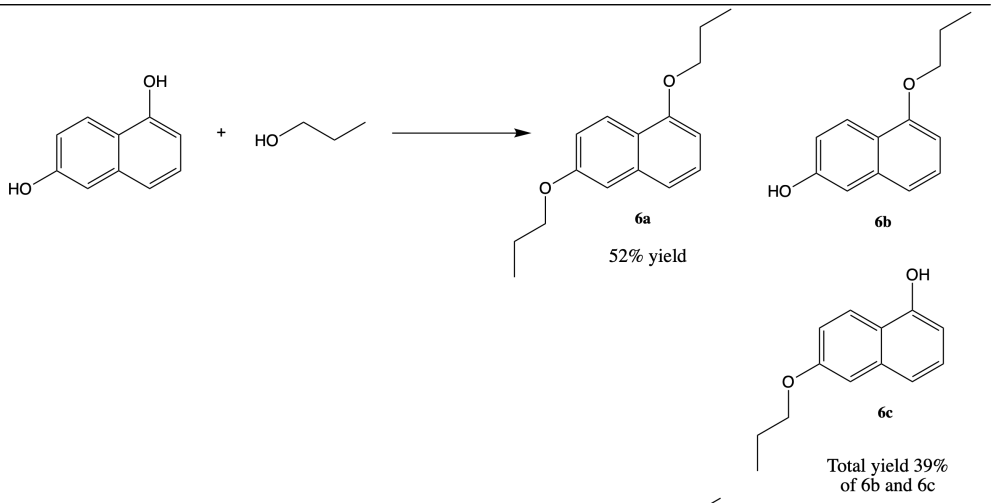
7	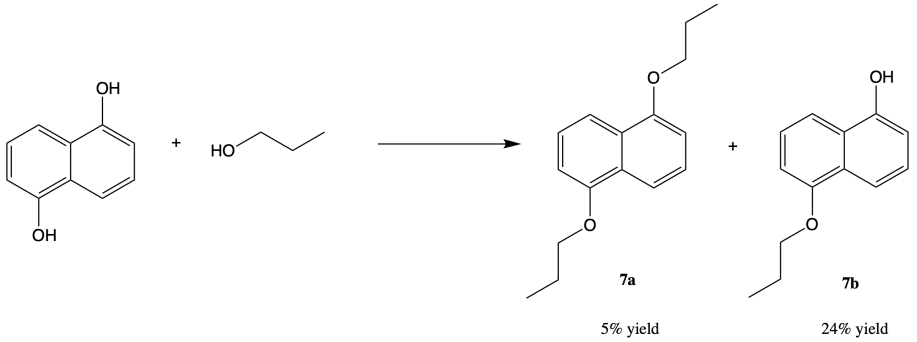
8	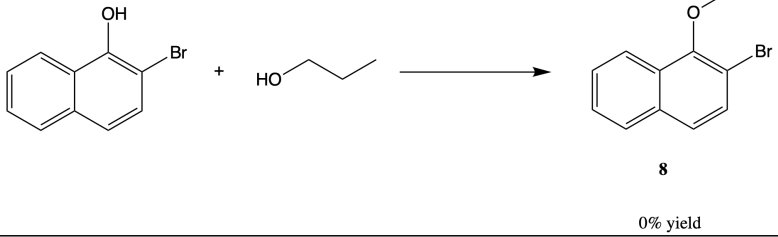

1-Propoxynaphthalene 4. The general procedure was followed on a 1 mmol scale to obtain 102 mg of the product as a yellow oil (54% yield). ^{1}**H NMR** (400 MHz, $CDCl_3$): δ 8.33 (d, J = 9.8 Hz, 1H), 7.81 (d, J = 9.9 Hz, 1H), 7.53 - 7.48 (m, 2H), 7.45 - 7.37 (m, 2H), 6.82 (d, J = 7.3 Hz, 1H), 4.12 (t, J = 6.4 Hz, 2H), 2.02 - 1.94 (m, 2H), 1.17 (t, J = 7.4 Hz, 3H).

2-Propoxynaphthalene 5. The general procedure was followed on a 1 mmol scale to obtain 132 mg of the product as a yellow oil (71% yield). ^{1}**H NMR** (400 MHz, $CDCl_3$): δ 7.78 - 7.70 (m, 3H), 7.43 (t, J = 6.8 Hz, 1H), 7.32 (t, J = 6.8 Hz, 1H), 7.14 (d, J = 11.1 Hz, 2H), 4.04 (t, J = 6.6 Hz, 2H), 1.93 - 1.84 (m, 2H), 1.09 (t, J = 7.4 Hz, 3H).

1,6-Dipropoxynaphthalene 6a. The general procedure was followed on a 1 mmol scale to obtain 126 mg of the di-substituted product **6a** as a white solid (52% yield) and 79 mg of the mono-substituted products **6b** and **6c** as a white solid (39% yield).

For **6a**: ^{1}**H NMR** (400 MHz, $CDCl_3$): δ 8.19 (d, J = 9.0 Hz, 1H), 7.33 - 7.28 (m, 2H),

7.13 - 7.08 (m, 2H), 6.66 (d, J = 5.9 Hz, 1H), 4.10 - 4.02 (m, 4H), 1.98 - 1.83 (m, 4H), 1.14 - 1.06 (m, 6H).

For mixture of **6b and 6c**: ^{1}**H NMR** (400 MHz, $CDCl_3$): δ 8.21 (d, J = 9.0 Hz, 1H), 8.07 (d, J = 9.1 Hz, 1H), 7.33 - 7.22 (m, 4H), 7.15 - 7.03 (m, 4H), 6.65 (d, J = 7.2 Hz, 2H), 5.15 (br s, 1H), 4.91 (br s, 1H), 4.09 - 4.02 (m, 4H), 1.97 - 1.83 (m, 4H), 1.21 (s, 2H), 1.16 - 1.06 (m, 7H), 0.94 - 0.86 (m, 2H).

1,5-Dipropoxynaphthalene 7a. The general procedure was followed on a 1 mmol scale to obtain 11 mg of the di-substituted product as a white solid (5% yield) and 48 mg of the mono-substituted product **7b** was obtained as a white solid (24% yield).

For **7a**: ^{1}**H NMR** (400 MHz, $CDCl_3$): δ 7.86 (d, J = 8.6 Hz, 2H), 7.35 (t, J = 8.0 Hz, 2H), 6.83 (d, J = 7.5 Hz, 2H), 4.09 (t, J = 6.4 Hz, 4H), 1.98 - 1.91 (m, 4H), 1.13 (t, J = 7.4 Hz, 6H).

For **7b**: ^{1}**H NMR** (400 MHz, $CDCl_3$): δ 7.90 (d, J = 8.4 Hz, 1H), 7.71 (d, J = 8.5 Hz, 1H), 7.38 (t, J = 7.6 Hz, 1H), 7.30 (t, J = 7.6 Hz, 1H), 6.84 (t, J = 5.2 Hz, 2H), 4.10 (t, J = 6.4 Hz, 2H), 2.0 - 1.91 (m, 2H), 1.13 (t, J = 7.4 Hz, 3H).

5.3 Preparation of aromatic linkers by *N*-arylation

***N*-Propylaniline 9.** To a round bottom flask, copper acetate ($Cu(OAc)_2$) (0.2 mmol, 36 mg) and BuOK (2 mmol, 224 mg) were added followed by propylamine (1 mmol, 0.082 mL), Bu_4NOH in 40% aqueous solution (2 mmol, 1.3 mL). At last, phenylboronic acid (1.5 mmol, 183 mg) was added as shown in Table 5.2. The reaction mixture was stirred at room temperature overnight. TLC was performed on the crude product (petroleum ether : ethyl acetate = 5:1). The reaction mixture was transferred to a separatory funnel together with distilled water (1 mL) and HCl (1 mL). The crude product was extracted with ethyl acetate (3 x 8 mL) three times. At last, the crude product was dried with sodium sulfate, filtrated and the solvent was evaporated. To isolate and purify the product, flash column chromatography was performed with a gradient of 0 to 5% ethyl acetate in petroleum ether. To analyze the product, ^{1}H NMR was used. No product was obtained.

Table 5.2: Reaction scheme for *N*-arylation catalyzed by copper.

Reaction	Reaction scheme
9	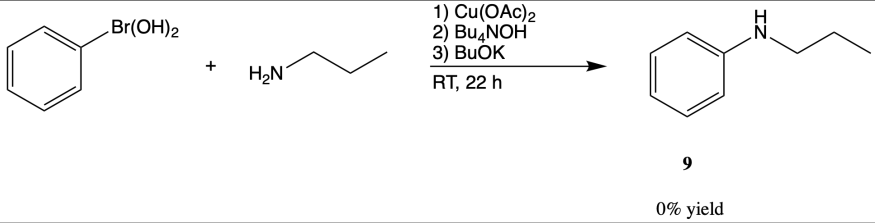 **9** 0% yield

5.4 Preparation of alkynes by Sonogashira coupling

In this experimental section, two different alkynes as presented in Table 5.3 were synthesized and used in further reactions to produce triazoles.

Table 5.3: Sonogashira reactions to produce alkynes used in further reactions.

Reaction	Reaction scheme
13	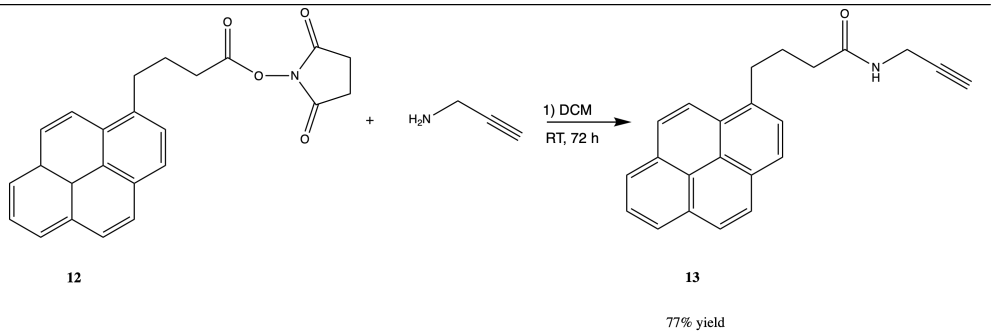 **12** **13** 77% yield
15	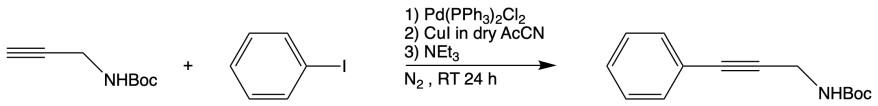 **15** 94% yield

***N*-(Prop-2-yn-1-yl)-4-(pyren-1-yl)butanamide 13.** To a 10 ml round bottom flask, PBASE **13** (0.3 mmol, 115 mg), propargylamine (3 mmol, 50 mg) and DCM (2 mL) were added. The reaction mixture was stirred at room temperature for 72 hours. To indicate if the product was obtained, TLC was performed on the crude product (petroleum ether : ethyl acetate = 1:1). The reaction mixture was transferred to a separatory funnel together with distilled water (10 mL) and ethyl acetate (25 mL) and the crude product was extracted with ethyl acetate (2 x 10 mL) two times. Next, the organic phase was washed with brine (5 mL) and additional ethyl acetate (5 mL). At last, the crude product was dried with sodium sulfate (Na_2SO_4), filtrated and the solvent was evaporated. To isolate and purify the product, flash column chromatography was performed with a gradient of 5 to 40% ethyl acetate in petroleum ether. To analyze the product, ^{1}H NMR was used.

The general procedure was followed on a 0.3 mmol scale to obtain 98 mg of the product **13** as a yellow solid (77% yield). Then, the general procedure was followed on a 0.1 mmol scale to obtain 45 mg of the product **13** as a yellow solid (72% yield). **^{1}H NMR** (400 MHz, $CDCl_3$): δ 8.30 (d, J = 9.4 Hz, 1H), 8.18 - 8.11 (m, 4H), 8.03 (s, 2H), 8.0 (t, J = 7.7 Hz, 1H), 7.86 (d, J = 8.0 Hz, 1H), 5.53 (s, 1H), 4.05 (q, 2H), 3.41 (t, J = 7.0 Hz, 2H), 2.31 - 2.21 (m, 5H).

***tert*-Butyl(3-phenylprop-2-yn-1-yl)carbamate 15.** The dry reagents *tert*-butyl prop-2-yn-1-ylcarbamate (2 mmol, 310 mg), $Pd(PPh_3)Cl_2$ (0.023 mmol, 16.56 mg) and copper(I)-iodide (0.046, 8.74 mg) were added to a sealed two-neck round bottom flask under dry nitrogen atmosphere. Then, iodobenzene (2.07 mmol, 0.23 mL) and dry acetonitrile (5 mL) were added. The solution was cooled to 0°C by putting the round bottom flask in an

ice bath. At 0°C, NEt_3 (4.14 mmol, 0.58 mL) was added and then the reaction mixture was allowed to warm to room temperature while stirred overnight. TLC was performed on the crude product (petroleum ether : ethyl acetate = 9:1) to see if the reaction was done. Next, the solvent was evaporated and the crude product was purified using flash column chromatography with a gradient of 0 to 10 % ethyl acetate in petroleum ether. At last, ^{1}H NMR was used to analyze the product.

The general procedure was followed on a 2 mmol scale to obtain 437 mg of the product **15** as a brown solid (94 % yield). **^{1}H NMR** (400 MHz, $CDCl_3$): δ 7.43 - 7.38 (m, 2H), 7.33 - 7.29 (m, 3H), 4.76 (s, 1H), 4.15 (s, 2H), 1.47 (s, 9H).

5.5 Preparation of triazoles by cycloaddition

A few single triazole units, **10**, **11**, **14** and **16** as well as a triazole-dimer **20** were prepared by performing CuAAC and RuAAC click-reactions between an alkyne and an organic azide. The reaction schemes are presented in Table 5.4.

Table 5.4: Click-reactions via RuAAC and CuAAC to produce di-substituted triazoles.

Reaction	Reaction scheme
10	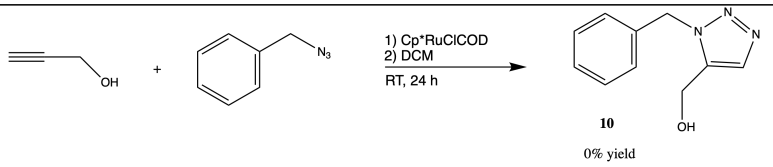 0% yield
11	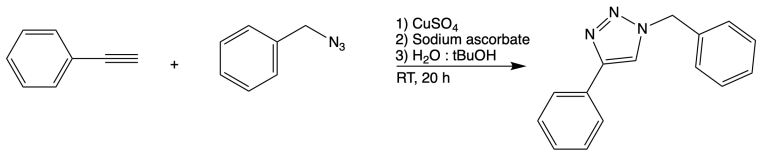 Product obtained No yield calculated
14A	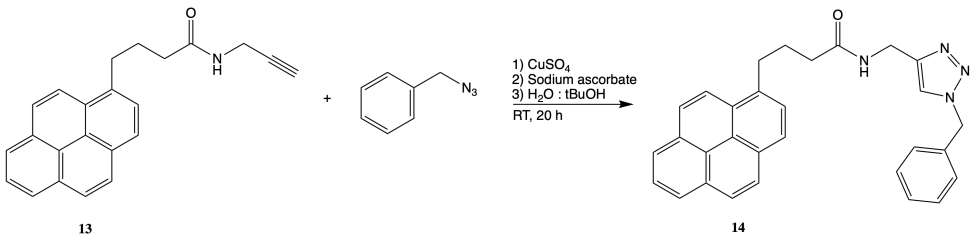 0% yield
14B	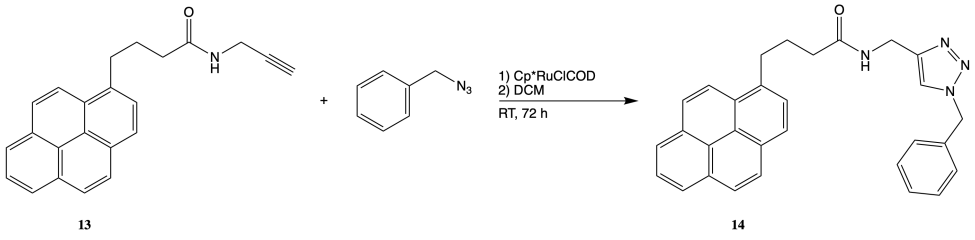 0% yield

Continued on next page

Table 5.4 – continued from previous page

Reaction	Reaction scheme
16	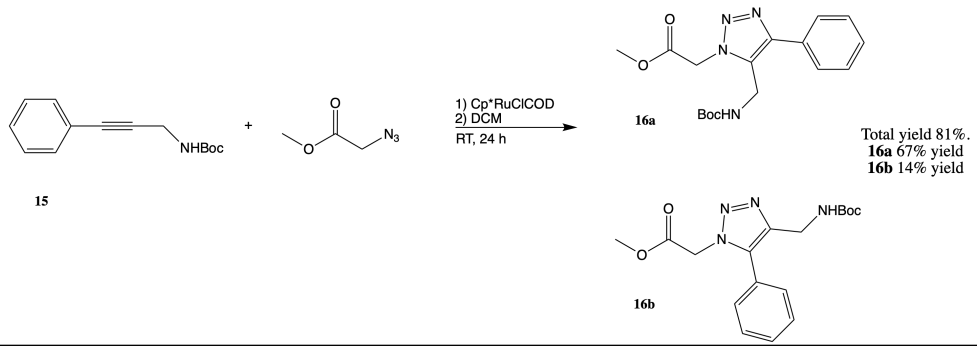

(1-Benzyl-1H-1,2,3-triazol-5-yl)methanol 10. The catalyst [Cp*RuCl(COD)] (0.02 mmol, 7.6 mg) was dissolved in anhydrous DCM (7.5 mL) in a two-neck round bottom flask under dry nitrogen atmosphere. Next, propargyl alcohol (1 mmol, 0.06 mL) and benzyl azide (1 mmol, 0.13 mL) were added to the sealed round bottom flask. The reaction mixture was stirred overnight at room temperature. TLC was performed to see if the reaction was done (petroleum ether : ethyl acetate = 1:1). No product was detected.

1-Benzyl-4-phenyl-1H-1,2,3-triazole 11. To a two-neck round bottom flask, sodium ascorbate (0.024 mmol, 4.8 mg) and $CuSO_4$ (0.008 mmol, 1.27 mg) was added under dry nitrogen atmosphere. Then, *tert*-butanol (0.5 mL) and distilled water (0.5 mL) (1:1) were added followed by phenyl acetylene (0.4 mmol, 0.044 mL) and benzyl azide (0.4 mmol, 0.05 mL). The reaction mixture was allowed to stir at room temperature overnight. TLC was performed (petroleum ether : ethyl acetate = 1:1) to see if product had formed. Next, the reaction mixture was transferred to a separatory funnel together with brine (20 mL). The organic phase was extracted with ethyl acetate (3 x 20 mL) three times. Then, the crude product was dried with sodium sulfate, filtrated and evaporated. To purify the product, flash column chromatography was performed with a gradient of 10 to 20 % ethyl acetate in petroleum ether. The compound became a solid inside the chromatography equipment, so the gradient was changed to 0 to 5 % methanol in DCM. At last, ^{1}H NMR was used to analyze the product which was obtained but the yield could not be calculated.

The general procedure was followed on a 0.4 mmol scale and the product was obtained, however no yield could be calculated. ^{1}**H NMR** (400 MHz, $CDCl_3$): δ 7.80 (d, J = 8.1 Hz, 2H), 7.66 (s, 1H), 7.42 – 7.31 (m, 8H), 5.59 (s, 2H).

***N*-((1-Benzyl-1H-1,2,3-triazol-4-yl)methyl)-4-(pyren-1-yl)butanamide 14.**

General procedure A: The previously synthesized alkyne, **13**, (0.14 mmol, 45.3 mg) was added to a two-neck round-bottom flask under dry nitrogen atmosphere. Next, sodium ascorbate (0.06 eq., 1.65 mg) and $CuSO_4$ (0.02 eq., 0.44 mg) were added followed by benzyl azide (0.14 mmol, 0.017 mL). A solution of *tert*-butanol (2 mL) and distilled water (2 mL) (1:1) was added. The reaction mixture was stirred at room temperature overnight and then the reaction was checked using TLC (petroleum ether : ethyl acetate = 1:1). No product was obtained.

General procedure B: The alkyne, **13**, (0.23 mmol, 75.1 mg) was dissolved in anhydrous DCM (5 mL) and was added to a two-neck round bottom flask under dry nitrogen atmosphere. The catalyst [Cp*RuCl(COD)] (0.05 eq., 4.37 mg) followed by benzyl azide (0.23 mmol, 0.3 mL) were added. The reaction mixture was stirred at room temperature for 48 hours and then the reaction was checked using TLC (petroleum ether : ethyl acetate = 1:1). No product was obtained.

Methyl 2-(4-(((*tert*-butoxycarbonyl)amino)methyl)-5-phenyl-1H-1,2,3-triazol-1-yl)acetate 16a. The catalyst [Cp*RuCl(COD)] (0.05 eq., 75.6 mg) was added to a two-neck round bottom flask under dry nitrogen atmosphere and then dissolved in anhydrous DCM (4 mL). The previously synthesized alkyne, **15**, (1.9 mmol, 437.3 mg) and methyl azidoacetate (1.9 mmol, 0.19 mL) were then added. The reaction went on at room temperature with stirring overnight, and thereafter TLC was performed to see if the reaction was done (petroleum ether : ethyl acetate = 1:1). Further, the solvent was evaporated and the crude product was purified using flash column chromatography with a gradient from 10 to 40% ethyl acetate in petroleum ether. ^{1}H NMR was used to analyze the product.

The general procedure was followed on a 1.9 mmol scale to obtain 442 mg of the first isomer **16a** (67 % yield) and 94 mg of the second isomer **16b** (14 % yield). **^{1}H NMR** (400 MHz, $CDCl_3$): δ 7.67 (d, J = 6.9 Hz, 2H), 7.49 – 7.38 (m, 3H), 5.38 (app br s, 2H), 4.55 (d, J = 6.1 Hz, 2H), 3.83 (s, 3H), 3.81 (s, 2H), 1.43 (s, 9H).

5.6 Preparation of a triazole dimer

To prepare a dimer, a certain synthetic route was followed starting with two triazoles, one of which was Boc-deprotected and the other of which was hydrolyzed to form a carboxylic acid. Then, HATU-mediated amide coupling was performed.

Table 5.5: Synthesis of a dimer via Boc-deprotection and ester hydrolysis of the two triazole isomers followed by HATU-mediated amide coupling.

Reaction	Reaction scheme
17	
18	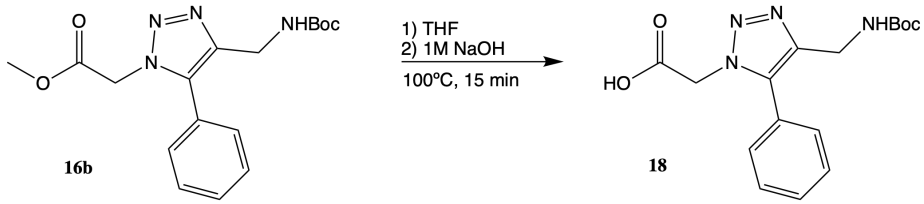

Continued on next page

Table 5.5 – continued from previous page

Reaction	Reaction scheme
19	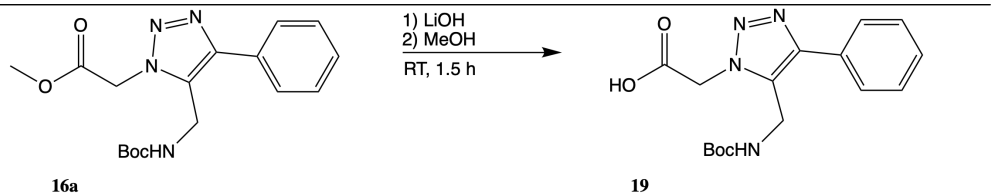
20	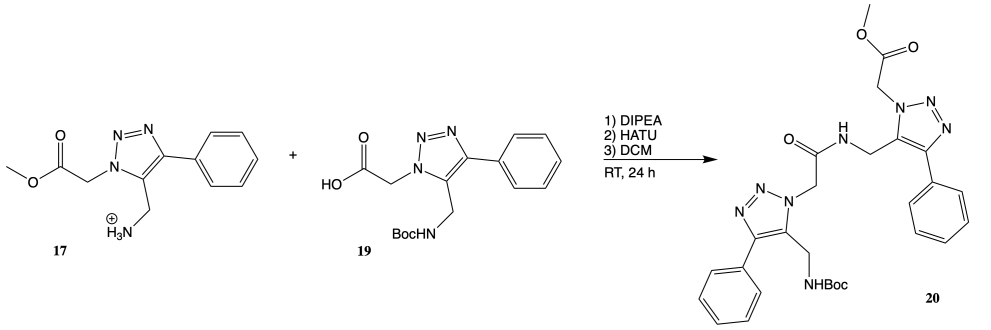

(1-(2-Methoxy-2-oxoethyl)-5-phenyl-1H-1,2,3-triazol-4-yl)methanaminium 17. For the deprotection of the amine, the first isomer **16a** (0.46 mmol, 153 mg) was dissolved in DCM (0.8 mL) and THF (11.6 eq., 0.4 mL) (2:1). The reaction mixture was stirred at room temperature for 1.5 hour. Then, the solvent was evaporated and the crude product was used directly in the next reaction to form a dimer.

2-(4-(((*tert*-Butoxycarbonyl)amino)methyl)-5-phenyl-1H-1,2,3-triazol-1-yl)acetic acid 18. For the ester hydrolysis, the second isomer **16b** (0.46 mmol, 153 mg) was dissolved in Me-THF (1.38 mL) in a vial. The vial was sealed and then NaOH (1.38 mmol, 1.38 mL) was added. The reaction mixture was placed in a microwave in which the solution was stirred for 50 seconds. The reaction proceeded for totally 15 minutes at 100 °C. Next, DCM (2 mL) was added to the vial followed by dropwise addition of HCl (1 M, 2 mL). The crude product was extracted with DCM (3 x 5 mL) three times and the dried over sodium sulfate, filtrated and evaporated. The product was used directly in the next reaction to form a dimer.

2-(5-(((*tert*-Butoxycarbonyl)amino)methyl)-4-phenyl-1H-1,2,3-triazol-1-yl)acetic acid 19. The first isomer **16a** (0.42 mmol, 145.5 mg) was dissolved in methanol (7 mL) in a round bottom flask and then LiOH (0.65 mmol, 0.65 mL) was added. The reaction mixture was stirred at room temperature for 1.5 hour. Distilled water (5 mL) was added followed by dropwise addition of 1 M HCl (0.6 mmol, 0.6 mL) while stirring. The product solution was transferred to a separating funnel and extracted with DCM four times (4 x 5 mL). The organic phase was dried with sodium sulfate, filtrated and the solvent was evaporated. The product was used directly in the next reaction to form a dimer.

Methyl 2-(4-(((2-(5-(((*tert*-butoxycarbonyl)amino)methyl)-4-phenyl-1H-1,2,3-triazol-1-yl)acetoxy)amino)methyl)-5-phenyl-1H-1,2,3-triazol-1-yl)acetate 20. HATU-mediated amide coupling: The Boc-deprotected triazole **17** (0.42 mmol, 145 mg) and the carboxylic acid **19** (0.42 mmol, 145 mg) were added to a vial and dissolved in DCM (8 mL). To the vial, HATU (0.42 mmol, 160 mg) was added followed by dropwise

addition of DIPEA (1.68 mmol, 0.28 mL). The reaction was stirred at room temperature overnight. Next, TLC was performed (petroleum ether : ethyl acetate = 1:2) to see if product had formed. The crude product was added to a separatory funnel together with NH_4Cl (8 mL) and then the organic phase was extracted with ethyl acetate (3 x 8 mL) three times. Further, the crude product was dried over $NaSO_4$, filtrated and evaporated. Flash column chromatography was performed with a gradient of 10 to 60 % ethyl acetate in petroleum ether to purify the product. ^{1}H NMR was used to analyze the product.

The general procedure was followed on a 0.42 mmol scale to obtain 12 mg of the dimer **20** as a white solid (5% yield). **^{1}H NMR** (400 MHz, $CDCl_3$): δ 7.61 (d, J = 7.1 Hz, 2H), 7.52 (d, J = 6.8 Hz, 2H), 7.46 (br s, 1H), 7.40 – 7.37 (m, 5H), 5.49 (br s, 1H), 5.32 (s, 2H), 5.05 (s, 2H), 4.68 (d, J = 5.6 Hz, 2H), 4.42 (d, J = 6.1 Hz, 2H), 3.72 (s, 3H), 1.42 (s, 9H).

5.7 Solvent effect on graphene

Seven different solvents; diethyl ether, DCM, ethanol, 1,4-dioxane, tetrahydrofuran, acetone and ethyl acetate, were investigated in four different experiments according to Table 5.6. The general procedure was followed to see how the solvents would affect graphene and the EVA/PET chip.

General procedure: Prior to the solvent experiments, the mobility of the graphene samples was measured by Hall-effect measurements. One or two graphene samples in each set were left as a reference control sample to see if external factors like transportation would affect the samples. The other graphene samples were put into separate dry vials and the different solvents (0.6 mL) were added in each vial, which was sealed and left for two hours. Then, the samples were taken out and dried with N_2 gas. The mobility was measured once again directly after the experiment. Next, the samples were put into a chamber with constant flow of N_2 gas overnight. The mobility was measured again after this step. In the fourth test, only one solvent (diethyl ether) was tested and after the experiment, the samples were kept in a chamber at 60 °C and in N_2 gas overnight.

Table 5.6: Graphene samples treated in different solvents in separate vials (V). Four experiments were made. One or two samples were left as control samples.

Test 1		**Test 2**		**Test 3**		**Test 4**	
V	**Solvent**	**V**	**Solvent**	**V**	**Solvent**	**V**	**Solvent**
1	Control	1	Diethyl ether	1	Control	1	Diethyl ether
2	Diethyl ether	2	Control	2	Diethyl ether	2	Diethyl ether
3	DCM	3	Ethanol	3	Ethanol	3	Diethyl ether
4	Ethanol	4	1,4 dioxane	4	1,4 dioxane	4	Diethyl ether
5	1,4 dioxane	5	Acetone	5	Acetone	5	Diethyl ether
6	THF	6	EtOAc	6	EtOAc	6	Control
7	Acetone	-	-	-	-	-	-
8	EtOAc	-	-	-	-	-	-
9	Control	-	-	-	-	-	-

5.8 Attachment of synthesized aromatic units on the graphene surface

Four experiments to functionalize the graphene surface with nine different aromatic compounds were performed. The compounds tested were 1-propoxynaphthalene **4**, 2-propoxynaphthalene **5**, 1,6-dipropoxynaphthalene **6a**, 6-propoxynaphthalen-1-ol **6b**, 5-propoxynaphthalen-2-ol **6c**, 1,5-propoxynaphthalene **7a**, 5-propoxynaphthalen-1-ol **7b** and had previously been synthesised as shown in Table 5.1. Two commercially supplied compounds, PBASE **13** and 1-pyrenecarboxaldehyde **22** shown in Figure 3.9 were also tested.

General procedure: The mobility of each graphene sample was measured by Hall-effect measurements prior to the experiments. One graphene sample in each set was left as a control sample. To separate dry vials, the aromatic compounds (5 mM) were added and also diethyl ether (0.6 mL) according to Table 5.7. Then, one graphene sample was added into each vial. The vials were sealed and left for two hours at room temperature. Each graphene sample was taken out and in the first and fourth experiment the samples were washed with clean solvent to remove excessive compound. All samples were dried with N_2 gas. After keeping the samples in a chamber at 60 °C and under constant flow of N_2 gas overnight, the mobility was measured again. In addition to the mobility measurements, Raman spectroscopy was used in the third and fourth experiment in Table 5.8 prior to and after the experiment.

Table 5.7: Different aromatic compounds dissolved in diethyl ether to bind to graphene samples by non-covalent interactions.

Test 1						
Vial	**Compound**	**V (mL)**	**C (mM)**	**n (mmol)**	**M (g/mol)**	**m (mg)**
1	**4**	0.6	5	0.003	186.25	0.558
2	**5**	0.6	5	0.003	186.25	0.558
3	**7b**	0.6	5	0.003	202.25	0.606
4	**7a**	0.6	5	0.003	244.33	0.733
5	**6a**	0.6	5	0.003	244.33	0.733
6	**6b, 6c**	0.6	5	0.003	202.25	0.606
7	**21**	0.6	5	0.003	230.27	0.691
8	Control	-	-	-	-	-
Test 2						
Vial	**Compound**	**V (mL)**	**C (mM)**	**n (mmol)**	**M (g/mol)**	**m (mg)**
1	**4**	0.6	5	0.003	186.25	0.558
2	**5**	0.6	5	0.003	186.25	0.558
3	**7b**	0.6	5	0.003	202.25	0.606
4	**6a**	0.6	5	0.003	244.33	0.733
5	**6b, 6c**	0.6	5	0.003	202.25	0.606
6	**12**	0.6	5	0.003	385.42	1.1562
7	**21**	0.6	5	0.003	230.27	0.691
8	Control	-	-	-	-	-

Table 5.8: Different aromatic compounds dissolved in diethyl ether to bind to graphene samples by non-covalent interactions. Raman spectroscopy was used prior to and after the two experiments.

Test 3						
Vial	**Compound**	**V (mL)**	**C (mM)**	**n (mmol)**	**M (g/mol)**	**m (mg)**
1	**4**	0.6	5	0.003	186.25	0.558
2	**5**	0.6	5	0.003	186.25	0.558
3	**7b**	0.6	5	0.003	202.25	0.606
4	**6a**	0.6	5	0.003	244.33	0.733
5	**6b, 6c**	0.6	5	0.003	202.25	0.606
6	**12**	0.6	5	0.003	385.42	1.1562
7	Control	-	-	-	-	-
Test 4						
Vial	**Compound**	**V (mL)**	**C (mM)**	**n (mmol)**	**M (g/mol)**	**m (mg)**
1	**4**	0.6	5	0.003	186.25	0.558
2	**5**	0.6	5	0.003	186.25	0.558
3	**7b**	0.6	5	0.003	202.25	0.606
4	**6a**	0.6	5	0.003	244.33	0.733
5	**6b, 6c**	0.6	5	0.003	202.25	0.606
6	**12**	0.6	5	0.003	385.42	1.1562
7	Control	-	-	-	-	-

Bibliography

[1] T. E. Nagel, B. K. Chan, D. De Vos, A. El-Shibiny, E. K. Kang'ethe, A. Makumi, and J. P. Pirnay. The Developing World Urgently Needs Phages to Combat Pathogenic Bacteria. *Front Microbiol.*, 882(7), 2016. doi: 10.3389/fmicb.2016.00882.

[2] Z. Jiang, B. Feng, J. Xu, T. Qing, P. Zhang, and Z. Qing. Graphene biosensors for bacterial and viral pathogens. *Biosensors and Bioelectronics*, 166(15):112471, October 2020. doi: 10.1016/j.bios.2020.112471.

[3] World Health Organization and the United Nations Children's Fund (UNICEF). A vision for primary health care in the 21st century: towards universal health coverage and the Sustainable Development Goals. WHO/HIS/SDS/2018.15 Licence: CC BY-NC-SA3.0 IGO 2018.

[4] T. Hone, J. Macinko, and C. Millett. Revisiting Alma-Ata: what is the role of primary health care in achieving the Sustainable Development Goals? *The Lancet*, 392(10156):1461–1472, 2018. doi: 10.1016/S0140-6736(18)31829-4.

[5] B. Smith. *Synthetic Receptors for Biomolecules: Design Principles and Applications*. The Royal Society of Chemistry, 2015. doi: 10.1039/9781782622062.

[6] N. Bhalla, P. Jolly, N. Formisano, and P. Estrela. Introduction to biosensors. *Essays in Biochemistry*, 60(1):1–8, June 2016. doi: 10.1042/EBC20150001.

[7] A. S. Stålsmeden J. R. Johansson, T. Beke-Somfai and N. Kann. Ruthenium-Catalyzed Azide Alkyne Cycloaddition Reaction: Scope, Mechanism, and Applications. *Chemical Reviews*, 23(116):14726–14768, February 2016. doi: 10.1021/acs.chemrev.6b00466.

[8] A. S. Stålsmeden, A. J. Paterson, I. Cs. Szigyártó, L. Thunberg, J. R. Johansson, T. Beke-Somfai, and N. Kann. Chiral 1,5-disubstituted 1,2,3-triazoles – versatile tools for foldamers and peptidomimetic applications. *Organic and Biomolecular Chemistry*, 18:1957–1967, February 2020. doi: 10.1039/D0OB00168F.

[9] B. Schulze and U. S. Schubert. Beyond click chemistry – supramolecular interactions of 1,2,3-triazoles. *Chemical Society Reviews*, 43(8):2522–2571, February 2014. doi: 10.1039/c3cs60386e.

[10] J. Clayden, N. Greeves, and S. Warren. *Organic Chemistry*. Oxford University Press, 2012. Retrieved January 18.

[11] J. Sherwood, J. H. Clark, I. J. S. Fairlamb, and J. M. Slattery. Solvent effects in palladium catalysed cross-coupling reactions. *Green Chemistry*, 21(9):2164 – 2213, 2019. doi: 10.1039/c9gc00617f.

[12] J. Björk, F. Hanke, C.-A. Palma, P. Samori, M. Cecchini, and M. Persson. Adsorption of aromatic and anti-aromatic systems on graphene through $\pi - \pi$-stacking. *The Journal of Physical Chemistry Letters.*, 1(23):3407–3412, November 2010. doi: 10.1021/jz101360k.

[13] Q. Ma, D. Chakraborty, F. Faglioni, R. P. Muller, W. A. Goddard, T. Harris, C. Campbell, and Y. Tang. Alkylation of Phenol: A Mechanistic View. *The Journal of Physical Chemistry*, 6(110):2246–2252, 2006. doi: 10.1021/jp0560213.

[14] C. Cazorla, É. Pfordt, M. C. Duclos, E. Métay, and M. Lemaire. O-Alkylation of phenol derivatives via a nucleophilic substitution. *Green Chemistry*, 13(9):2482 – 2488, August 2011. doi: 10.1039/c1gc15481h.

[15] M. Inagaki, F. Kang, M. Toyoda, and H. Konno. Chapter 3 - Graphene: Synthesis and Preparation. *Advanced Materials Science and Engineering of Carbon*, pages 41–65, 2014. doi: 10.1016/B978-0-12-407789-8.00003-X.

[16] J. Liu, Z. Liu, C. J. Barrow, and W. Yang. Molecularly engineered graphene surfaces for sensing applications: A review. *Analytica Chimica Acta*, 859:1–19, February 2015. doi: 10.1016/j.aca.2014.07.031.

[17] S. Giwan, L. Geonhee, J. Kim Mi, B. Seung-Hwa, and C. Minsuk. Rapid Detection of COVID-19 Causative Virus (SARS-CoV-2) in Human Nasopharyngeal Swab Specimens Using Field-Effect Transistor-Based Biosensor. *ACS Nano*, 14(4):5135–5142, 2020. doi: 10.1021/acsnano.0c02823.

[18] P. Zygouri, G. Potsi, E. Mouzourakis, K. Spyrou, D. Gournis, and P. Rudolf. Non-covalent Interactions of Graphene with Polycyclic Aromatic Hydrocarbons. *Current Organic Chemistry*, 19(18):1791–1799, August 2015. doi: 10.2174/1385272819666150526003634.

[19] Z. Gao, H. Xia, J. Zauberman, Ma. Tomaiuolo, J. Ping, and Q. Zhang. Detection of Sub-fM DNA with Target Recycling and Self-Assembly Amplification on Graphene Field-Effect Biosensors. *Nano Letters*, 18(6):3509–3515, 2018. doi: 10.1021/acs.nanolett.8b00572.

[20] C. Peng and X. Zhang. Chemical Functionalization of Graphene Nanoplatelets with Hydroxyl, Amino, and Carboxylic Terminal Groups. *Chemistry*, 3(3):873–888, August 2021. doi: 10.3390/chemistry3030064.

[21] S. Brülls. Non-covalent Modification of Graphene and MoS2. Synthesis and Characterization of Charged Molecules and Two-Dimensional Materials. *Chalmers University of Technology*, 2020. Retrieved February 11.

[22] J. O. Carlsson and P. M. Martin. Chapter 7 - Chemical Vapor Deposition in Handbook of Deposition Technologies for Films and Coatings. *Science, Applications and Technology*, pages 314–363, 2010. doi: 10.1016/B978-0-8155-2031-3.00007-7.

[23] M. Khan, K. Indykiewicz, P. Lam Tam, and A. Yurgens. High Mobility Graphene on EVA/PET. *Nanomaterials*, 12(3), 2022. doi: 10.3390/nano12030331.

[24] Z. Jiangab, Y. Zhanga, Y.-W. Tana, H. L. Stormerac, and P.Kima. Quantum Hall effect in graphene. *Solid State Communications*, 143(1-2):14–19, July 2007. doi: 10.1016/j.ssc.2007.02.046.

[25] L. Xu, S. Ramadan, and O. Akingbade. Detection of Glial Fibrillary Acidic Protein in Patient Plasma Using On-Chip Graphene Field-Effect Biosensors, in Comparison with ELISA and Single-Molecule Array. *ACS Sensors*, 7(1):253–262, 2022. doi: 10.1021/acssensors.1c02232.

A

^{1}H NMR spectra

1-Propoxynaphthalene

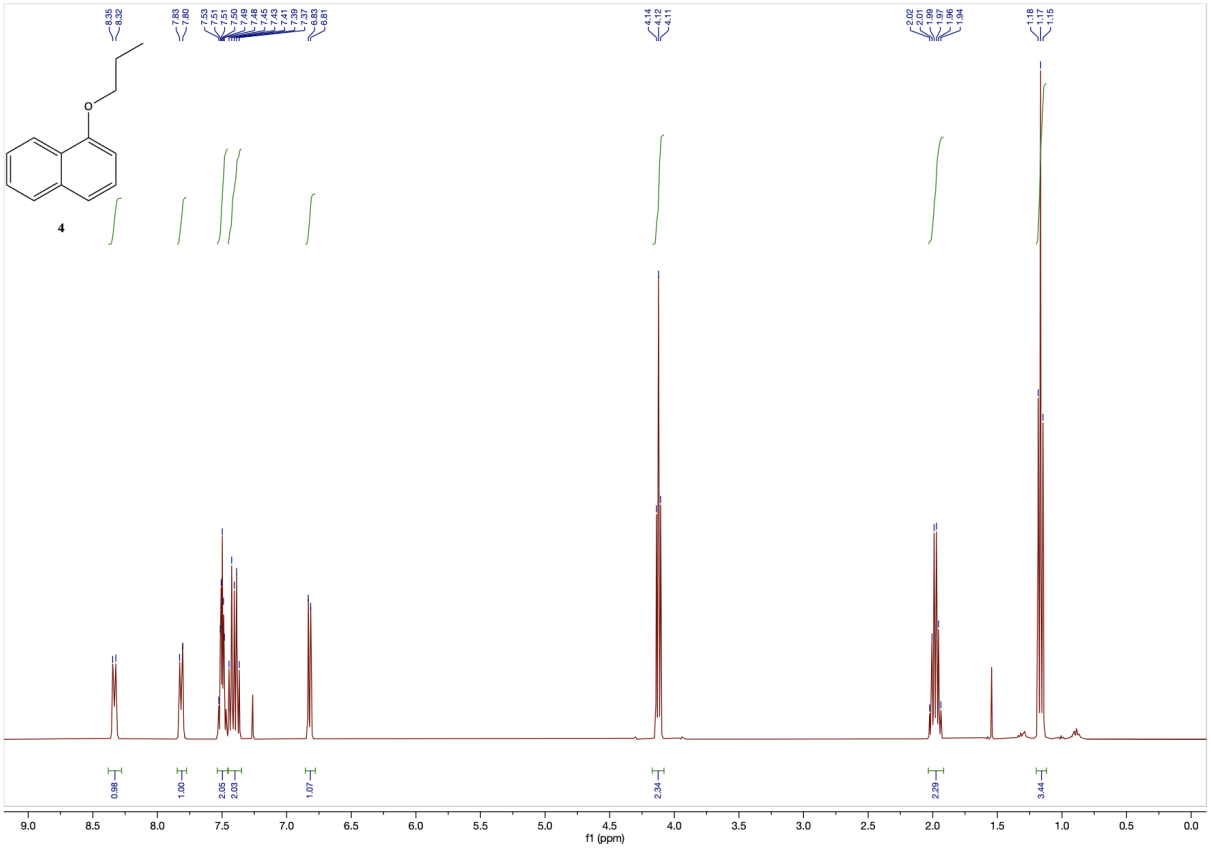

Figure A.1: ^{1}H NMR spectrum of the *O*-alkylated compound **4**.

2-Propoxynaphthalene

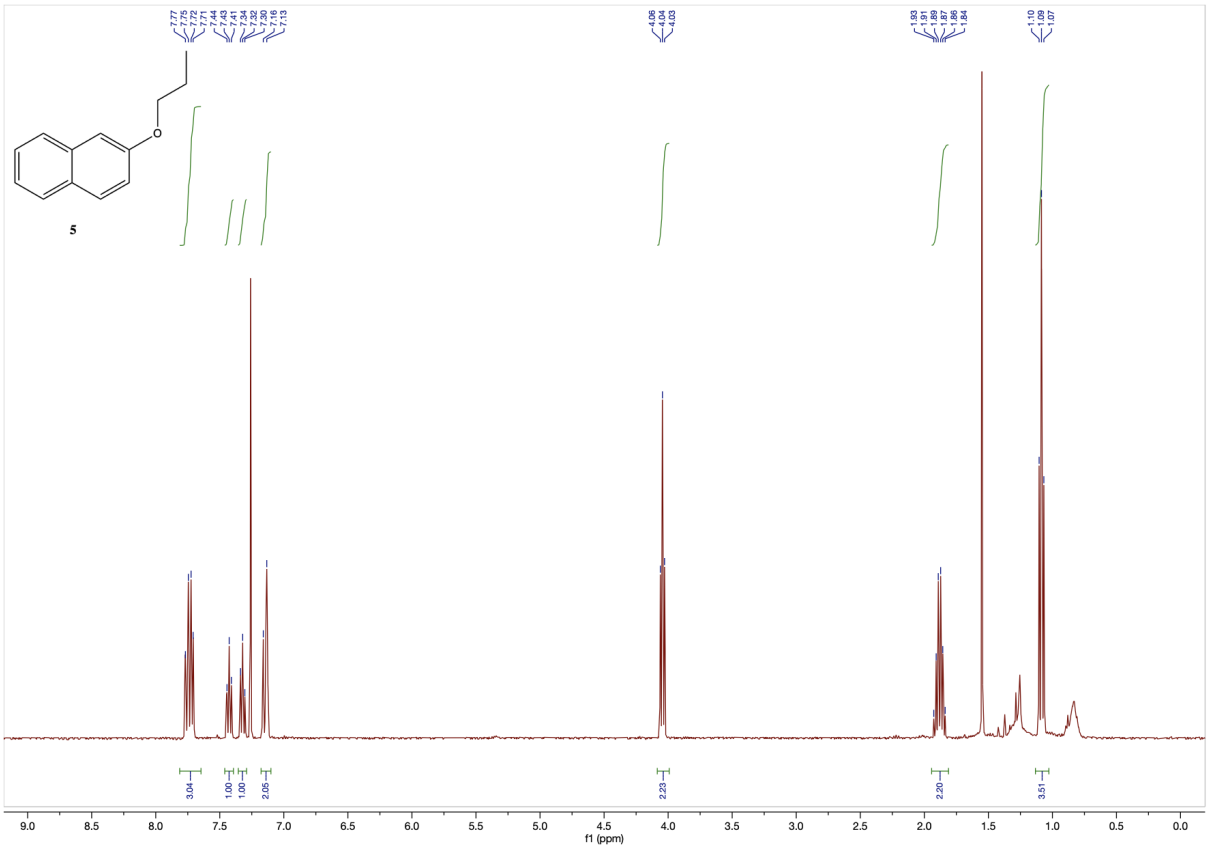

Figure A.2: ^{1}H NMR spectrum of the *O*-alkylated compound **5**.

1,6-Dipropoxynaphthalene

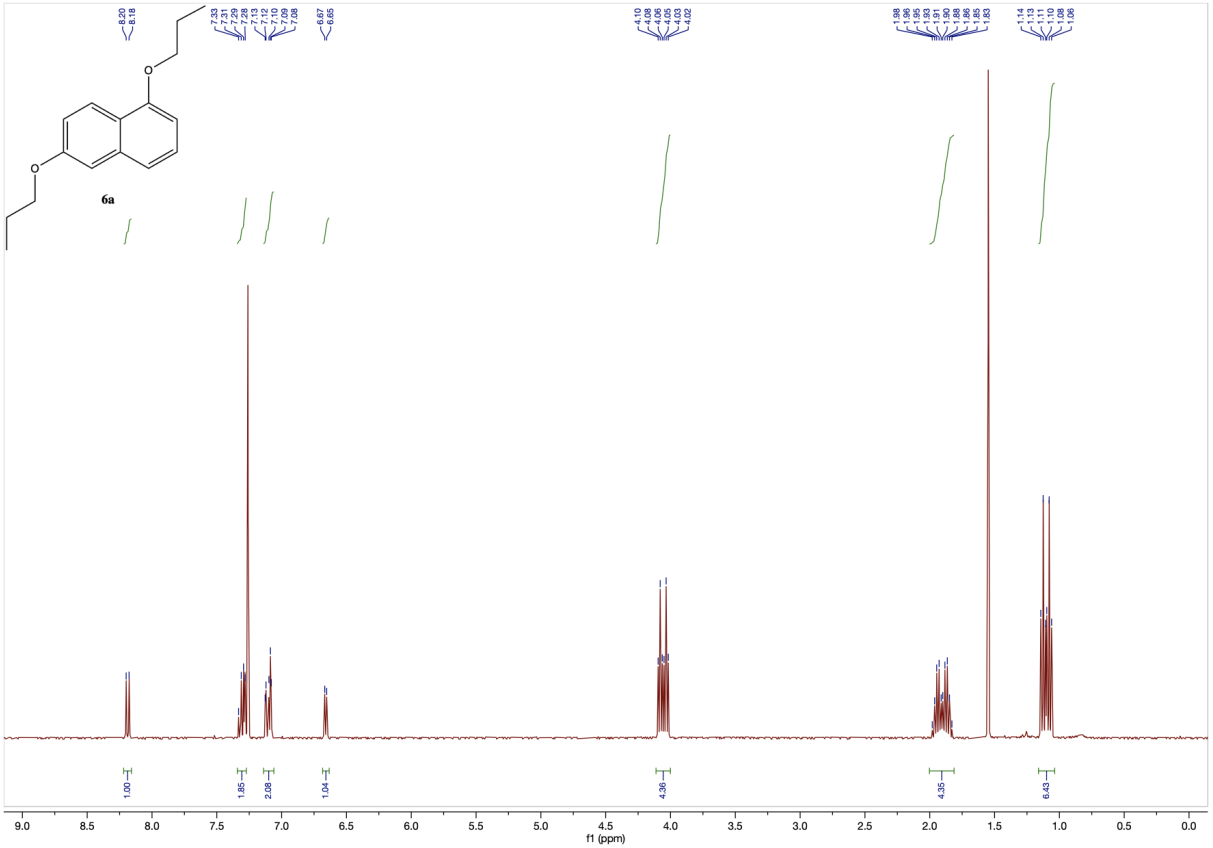

Figure A.3: ^{1}H NMR spectrum of the *O*-alkylated compound **6a**.

6-Propoxynaphthalene-1-ol and 5-Propoxynaphthalene-2-ol

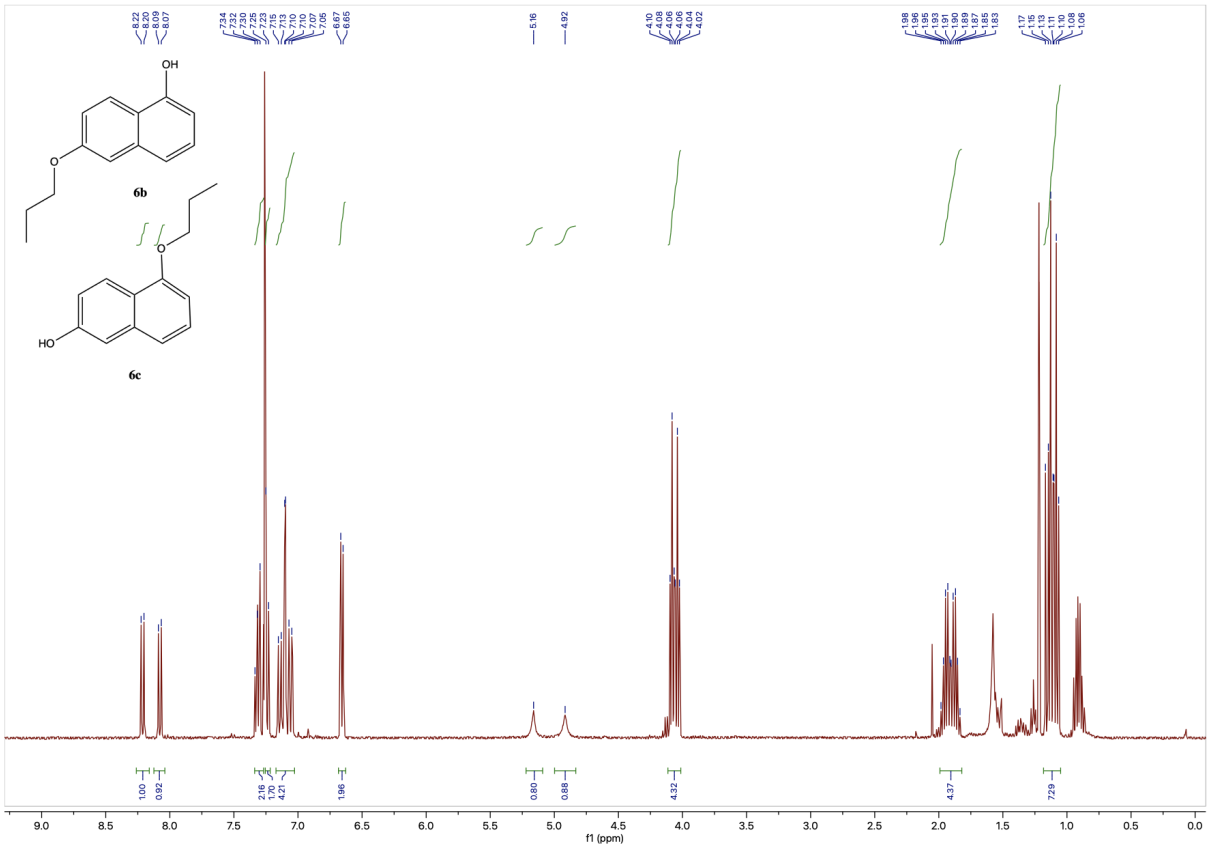

Figure A.4: ^{1}H NMR spectrum of the *O*-alkylated compounds **6b** and **6c**.

1,5-Dipropoxynaphthalene

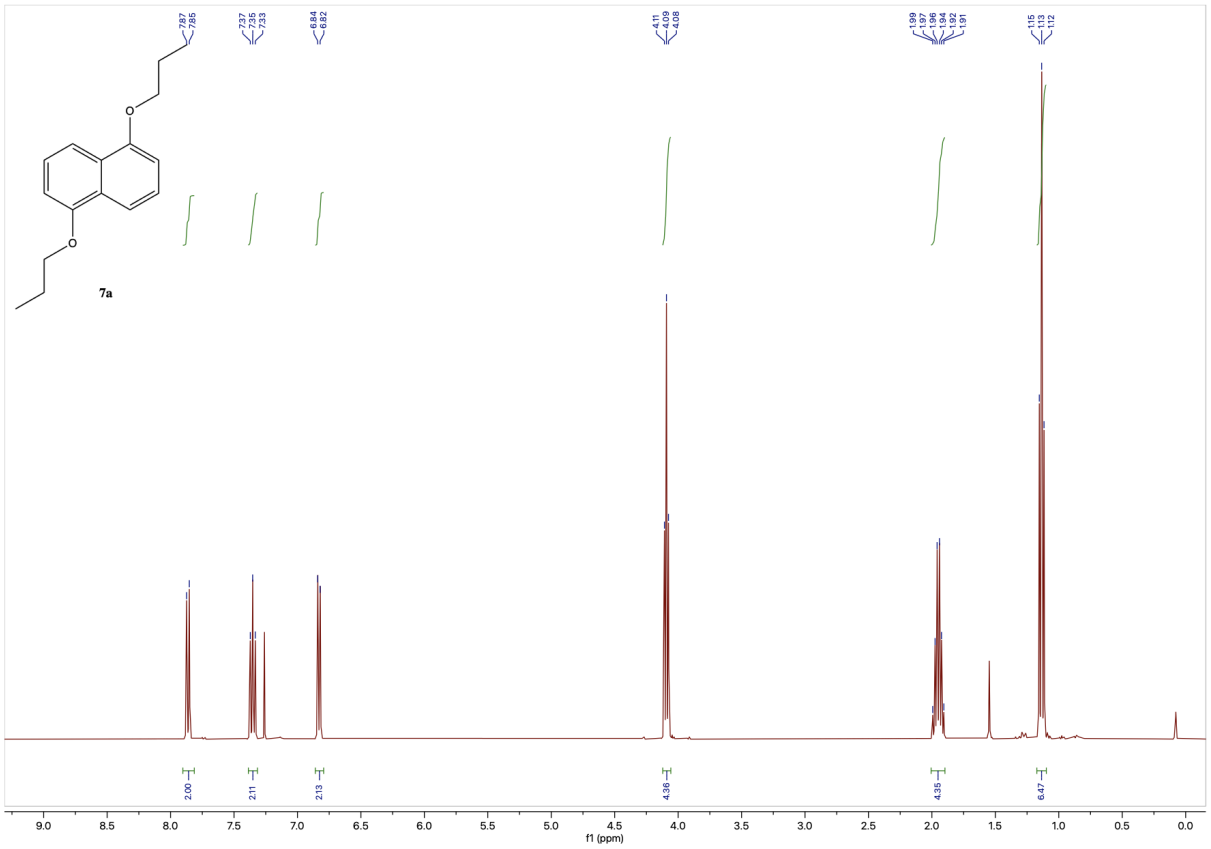

Figure A.5: ^{1}H NMR spectrum of the *O*-alkylated compound **7a**.

5-Propoxynaphthalene-1-ol

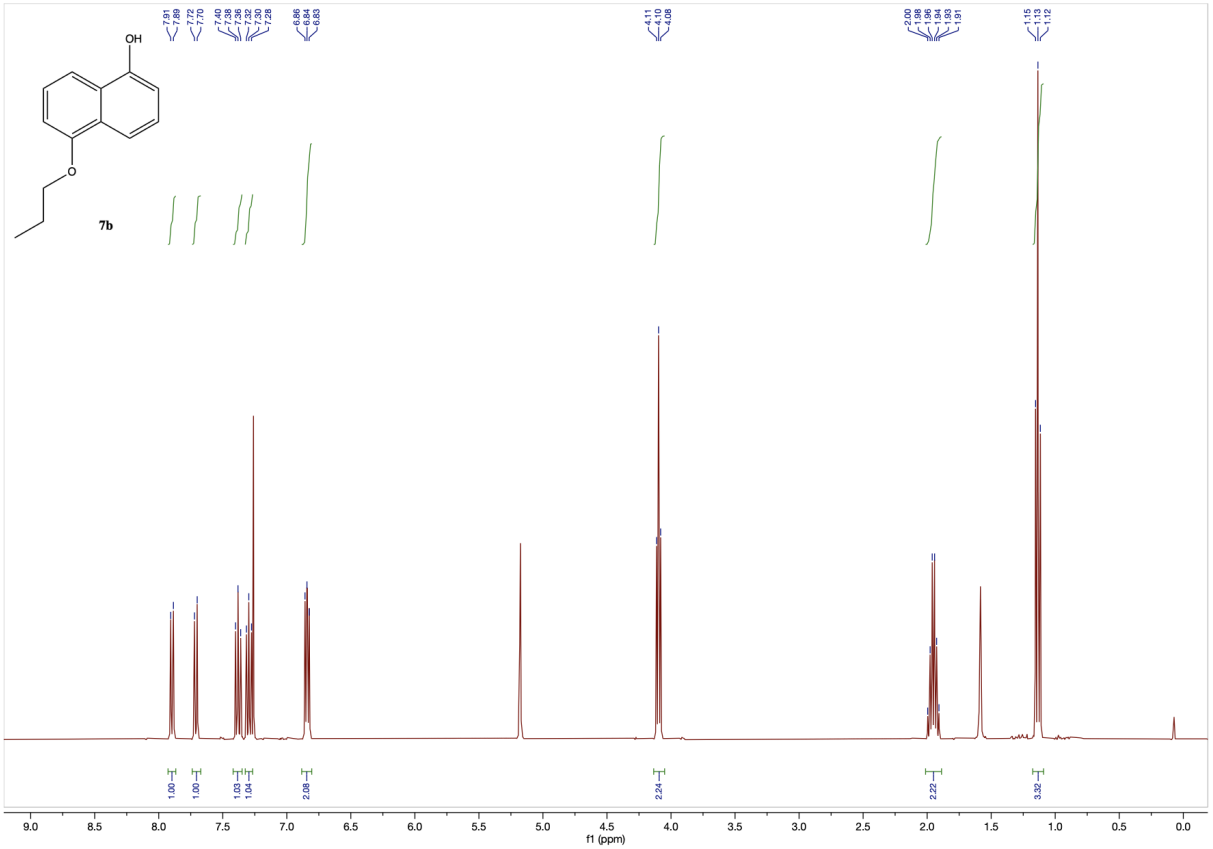

Figure A.6: ^{1}H NMR spectrum of the *O*-alkylated compound **7b**.

1-Benzyl-4-phenyl-1H-1,2,3-triazole

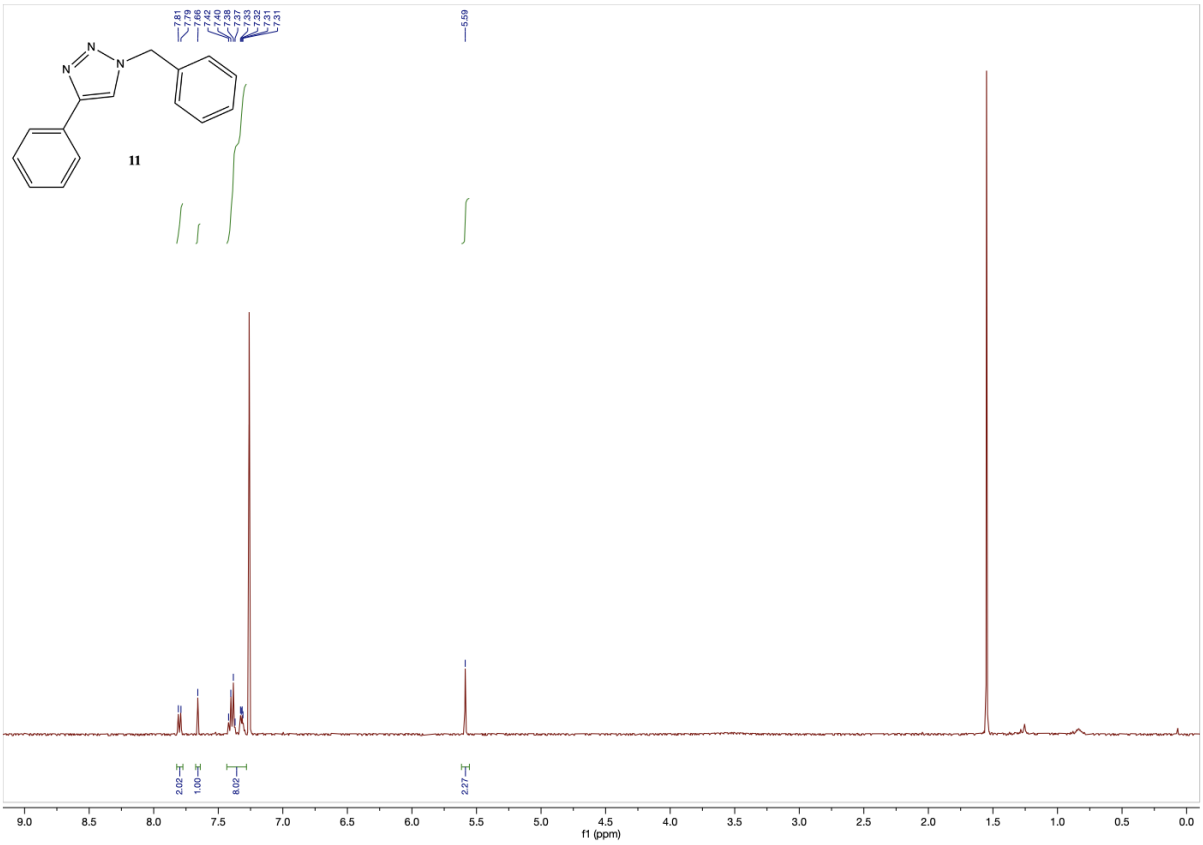

Figure A.7: ^{1}H NMR spectrum of the triazole **11**.

N-(Prop-2-yn-1-yl)-4-(pyren-1-yl)butanamide

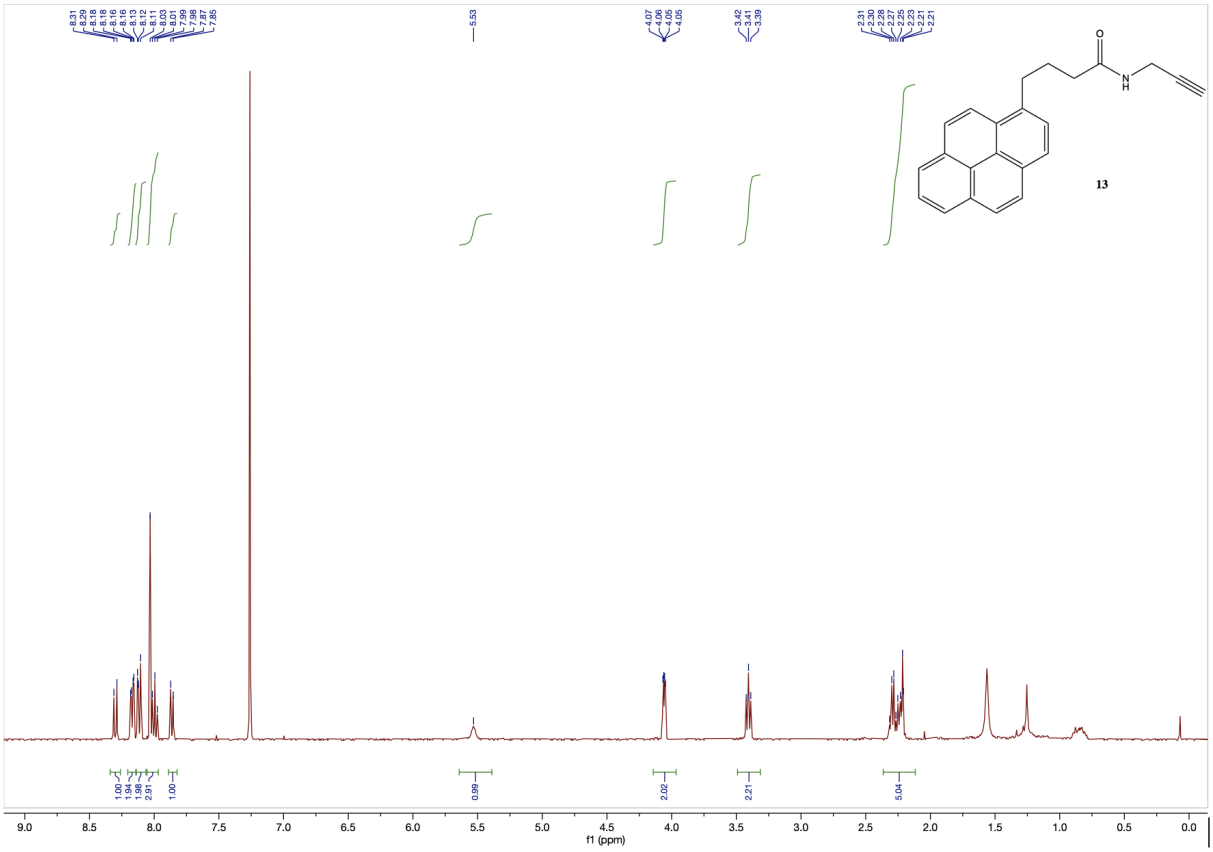

Figure A.8: ^{1}H NMR spectrum of the alkyne **13**.

tert-Butyl (3-phenylprop-2-yn-1-yl)carbamate

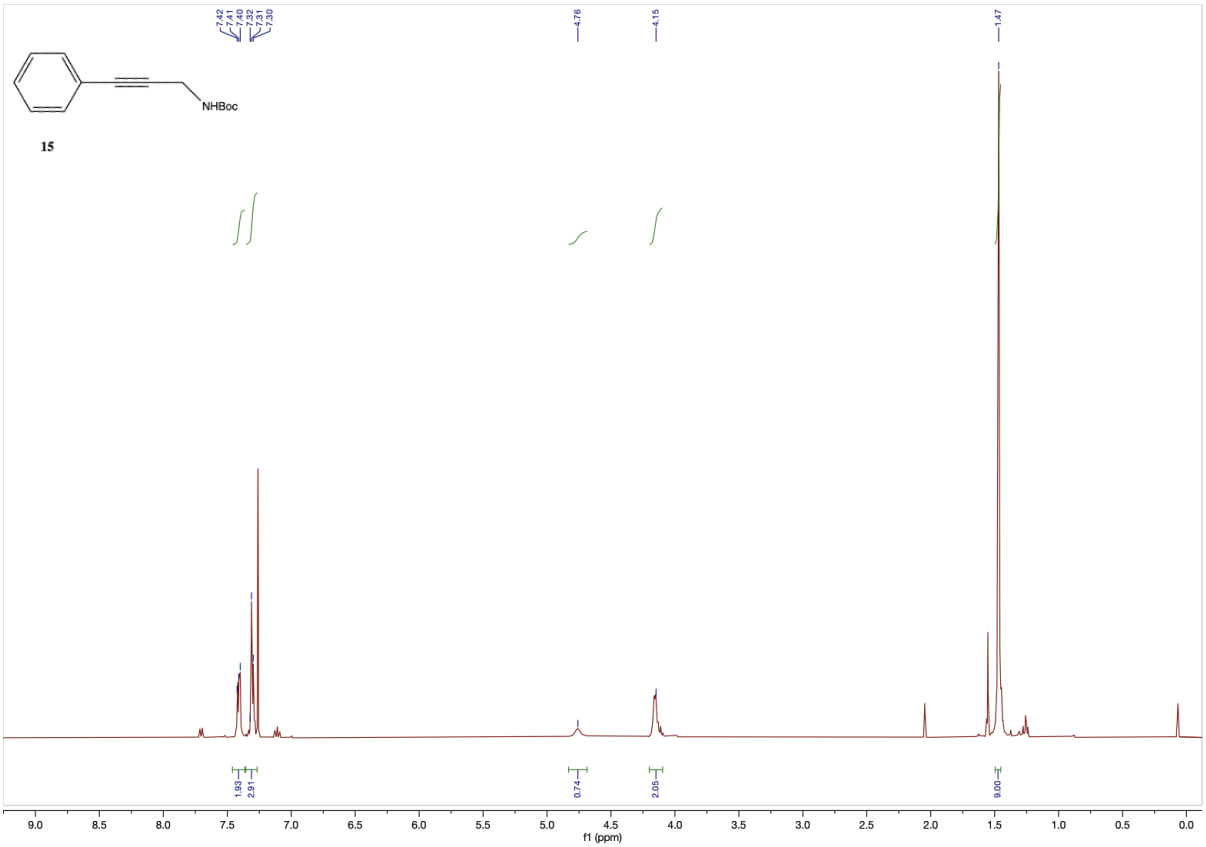

Figure A.9: ^{1}H NMR spectrum of the alkyne **15**.

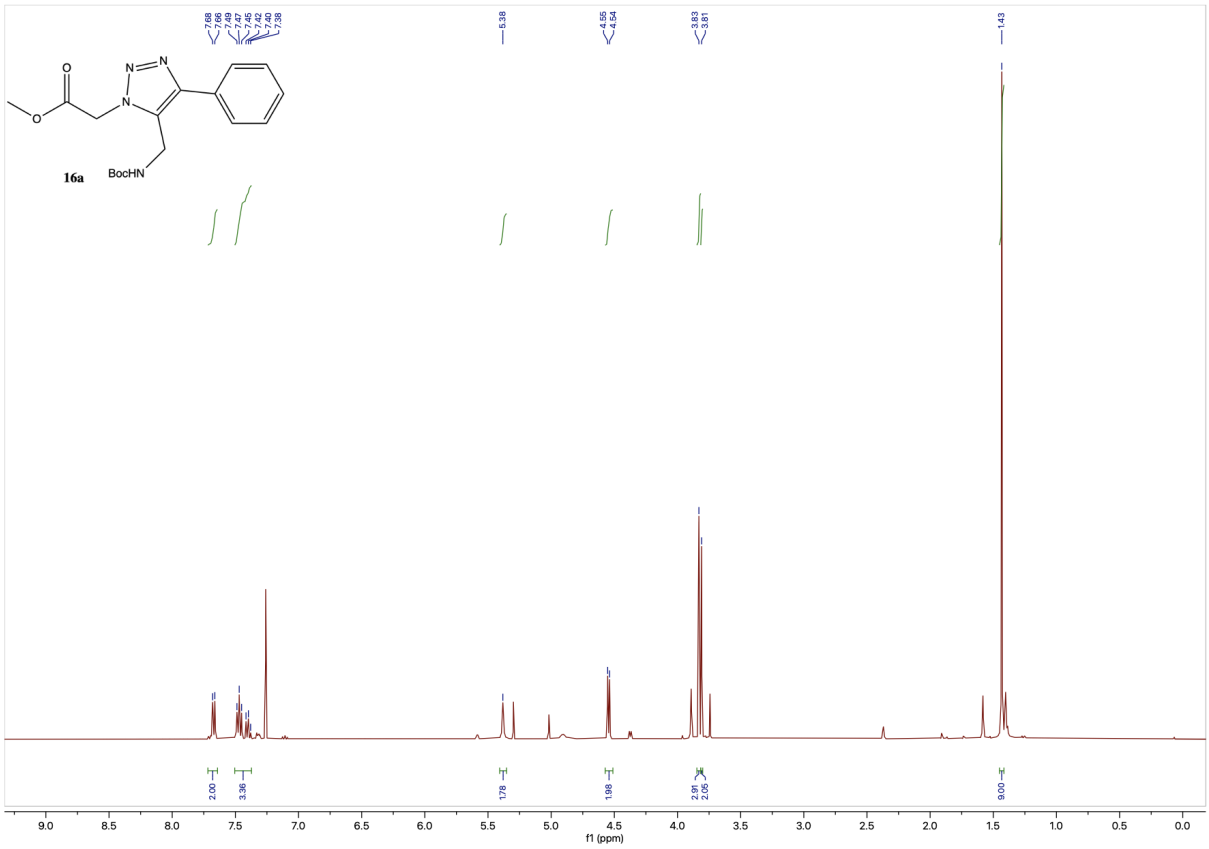

Figure A.10: ^{1}H NMR spectrum of the triazole compound **16a**.

Methyl 2-(4-(((2-(4-(((*tert*butoxycarbonyl)amino)methyl)-5-phenyl-1H-1,2,3triazol-1-yl)acetoxy)amino)methyl)-5-phenyl-1H-1,2,-3-triazol-1-yl)acetate

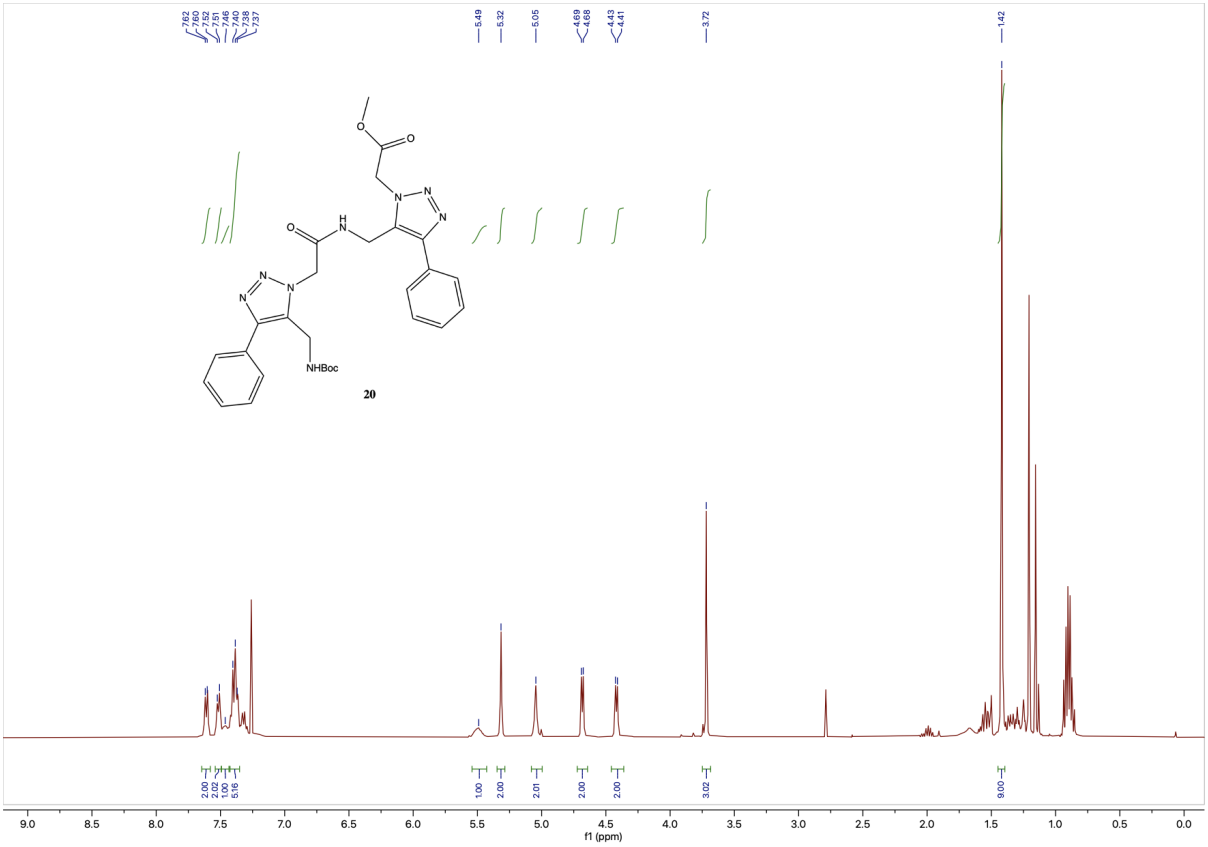

Figure A.11: ^{1}H NMR spectrum of the dimer **20**.

B

Raman spectra

1-Propoxynaphthalene

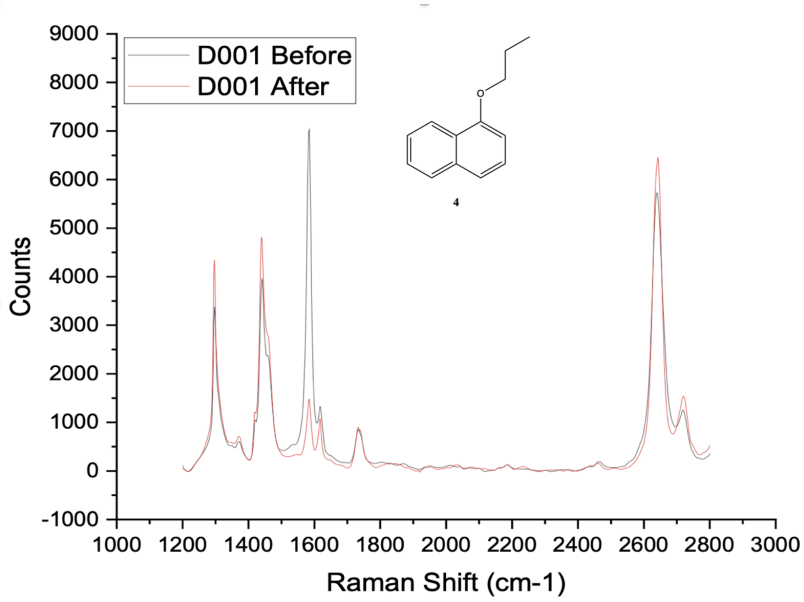

Figure B.1: Raman spectrum of the *O*-alkylated compound **4** in the third test.

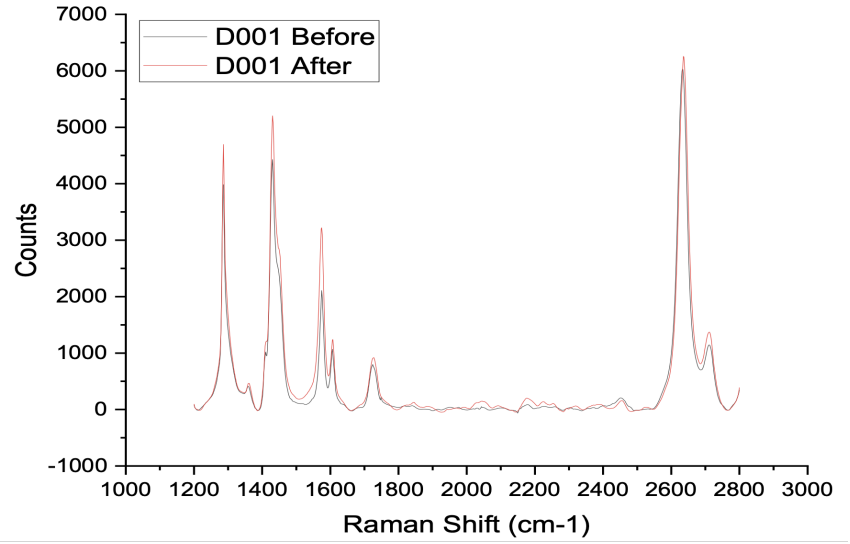

Figure B.2: Raman spectrum of the *O*-alkylated compound **4** in the fourth test.

2-Propoxynaphthalene

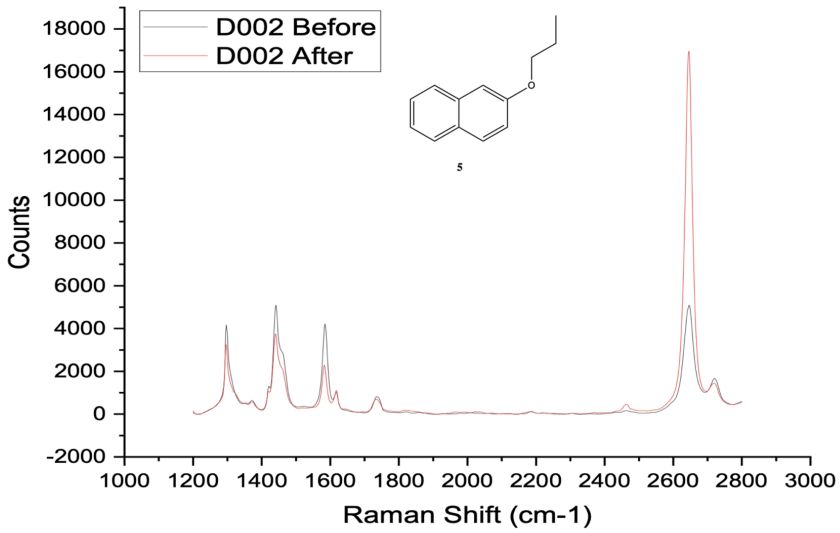

Figure B.3: Raman spectrum of the *O*-alkylated compound **5** in the third test.

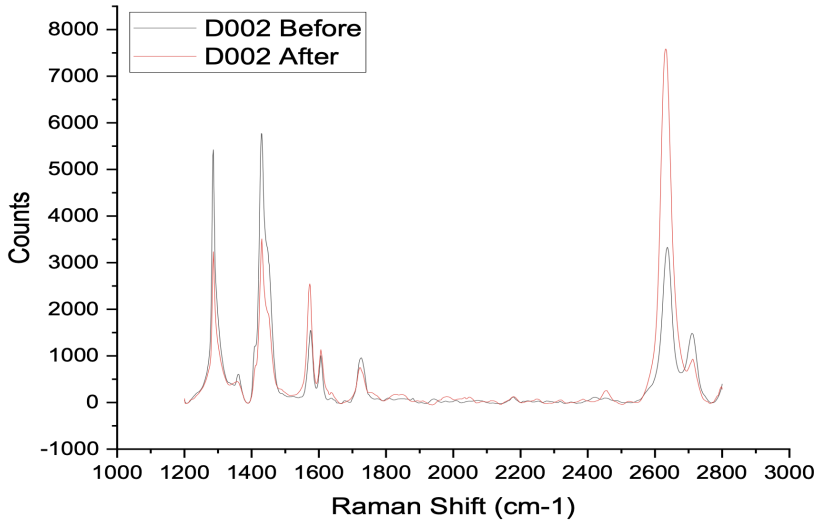

Figure B.4: Raman spectrum of the *O*-alkylated compound **5** in the fourth test.

5-Propoxynaphthalene-1-ol

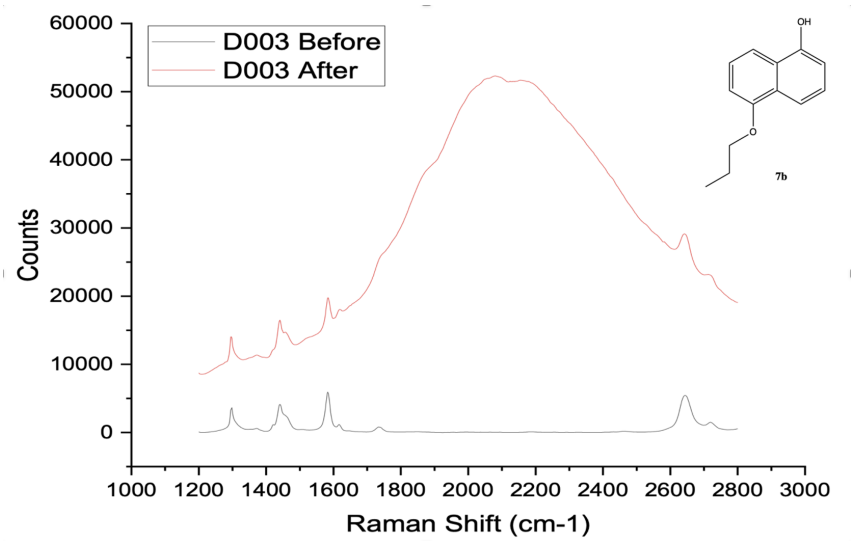

Figure B.5: Raman spectrum of the *O*-alkylated compound **7b** in the third test.

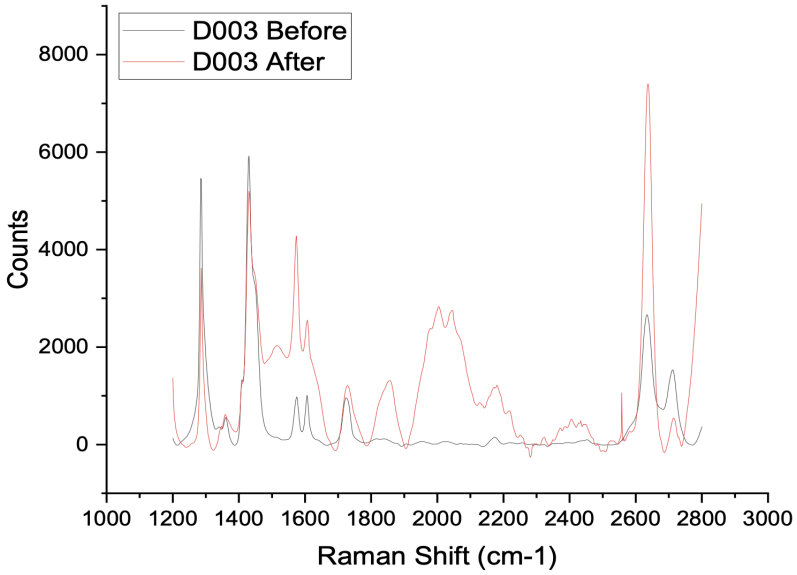

Figure B.6: Raman spectrum of the *O*-alkylated compound **7b** in the fourth test.

1,6-Dipropoxynaphthalene

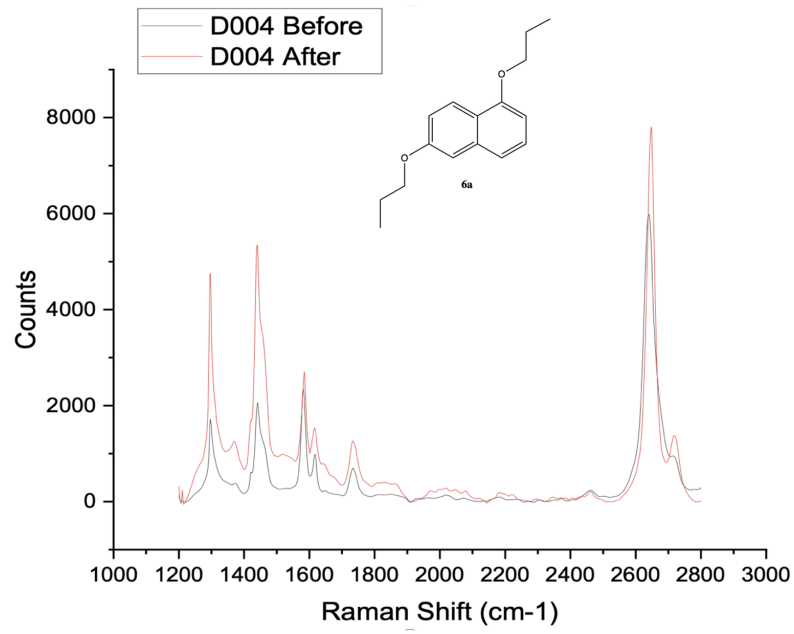

Figure B.7: Raman spectrum of the *O*-alkylated compound **6a** in the third test.

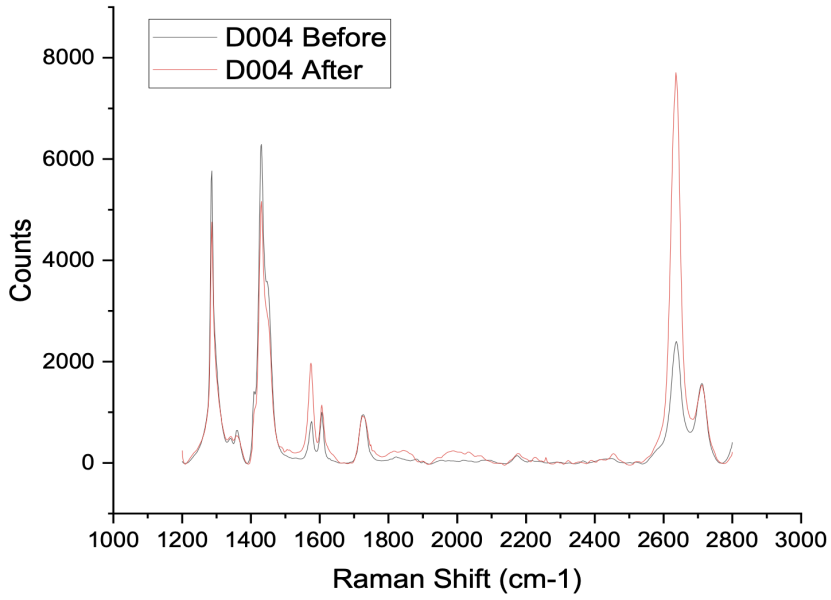

Figure B.8: Raman spectrum of the *O*-alkylated compound **6a** in the fourth test.

6-Propoxynaphthalene-1-ol & 5-Propoxynaphthalene-2-ol

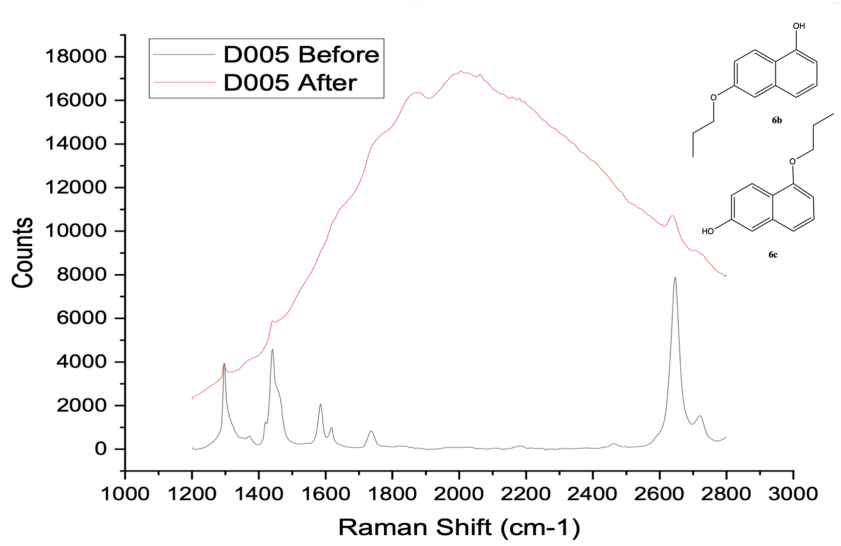

Figure B.9: Raman spectrum of the *O*-alkylated compounds **6b** and **6c** in the third test.

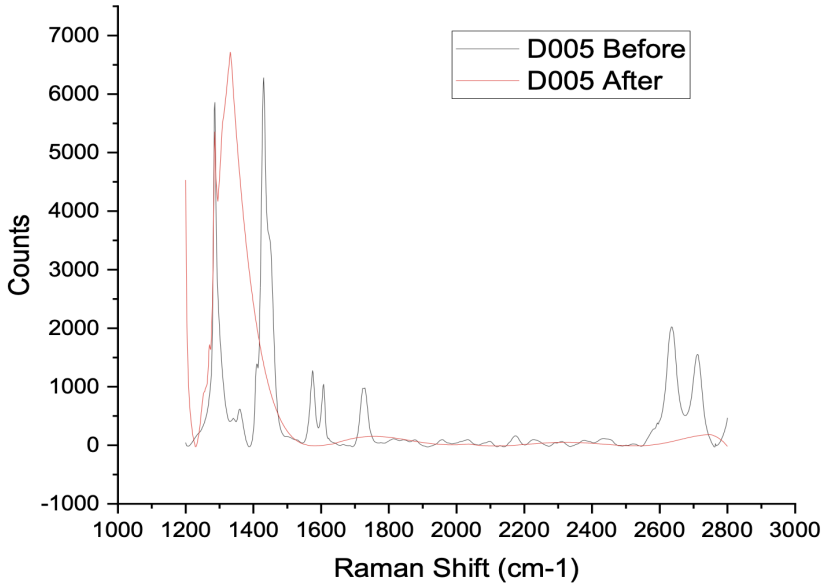

Figure B.10: Raman spectrum of the *O*-alkylated compounds **6b** and **6c** in the fourth test.

PBASE

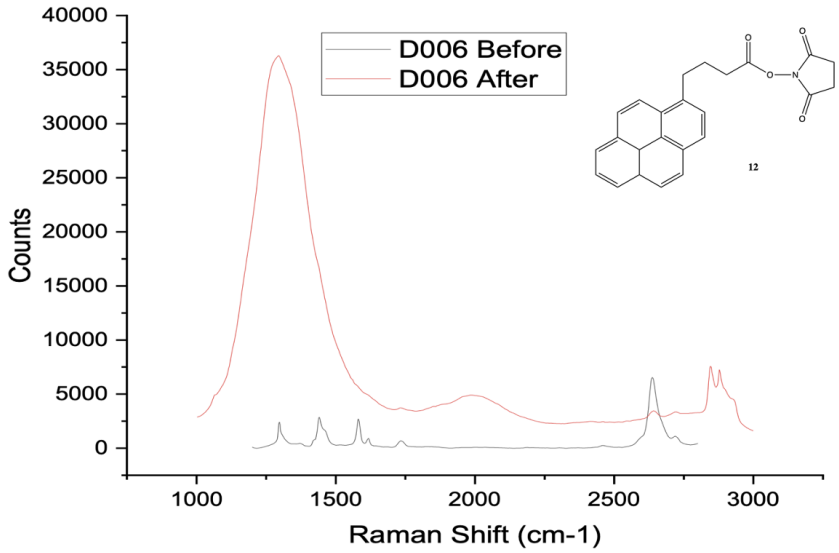

Figure B.11: Raman spectrum of PBASE **12** in the third test.

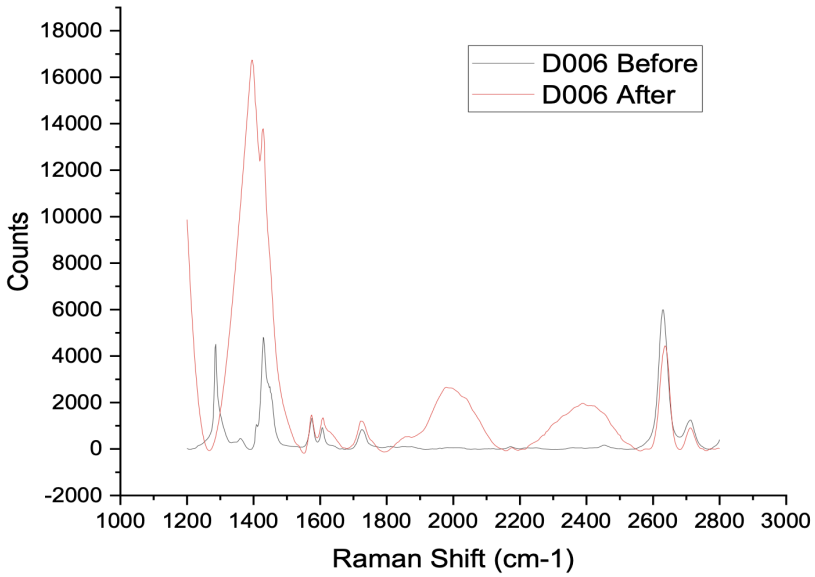

Figure B.12: Raman spectrum of PBASE **12** in the fourth test.

Control sample

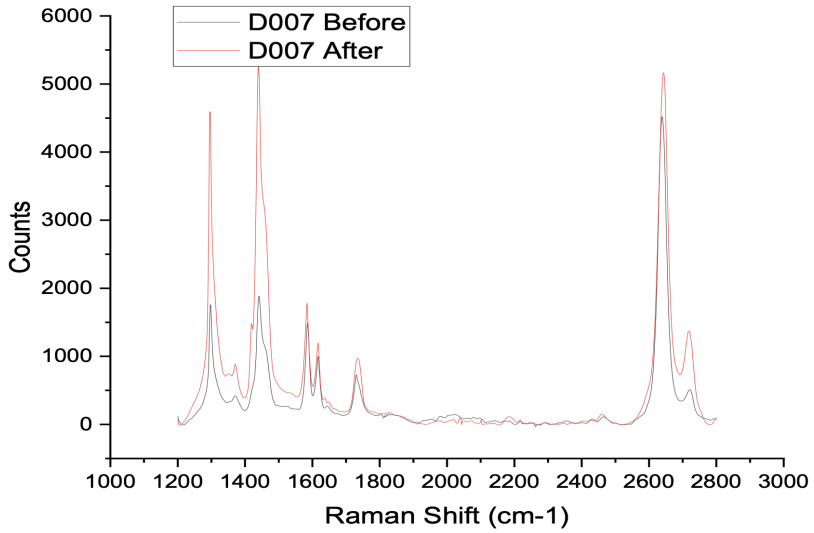

Figure B.13: Raman spectrum of the control sample in the third test.

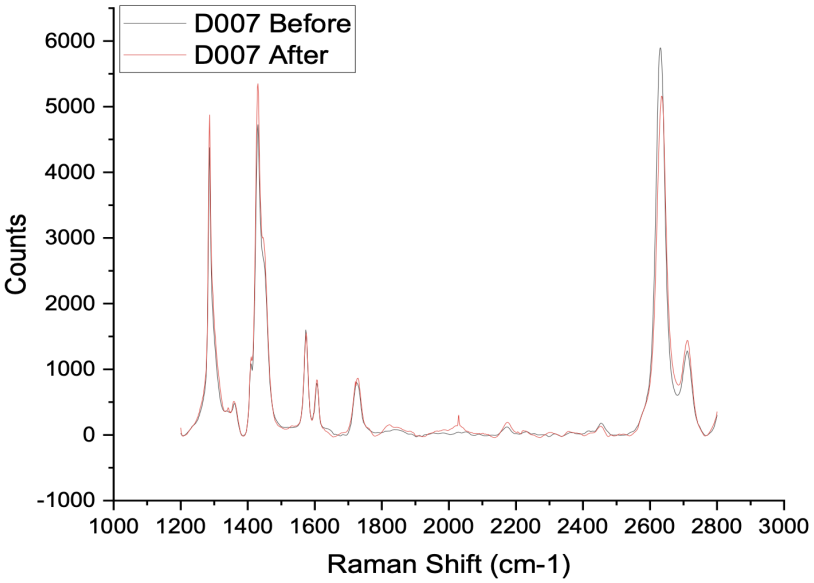

Figure B.14: Raman spectrum of the control sample in the fourth test.

DEPARTMENT OF SOME SUBJECT OR TECHNOLOGY
CHALMERS UNIVERSITY OF TECHNOLOGY
Gothenburg, Sweden
www.chalmers.se

CHALMERS
UNIVERSITY OF TECHNOLOGY